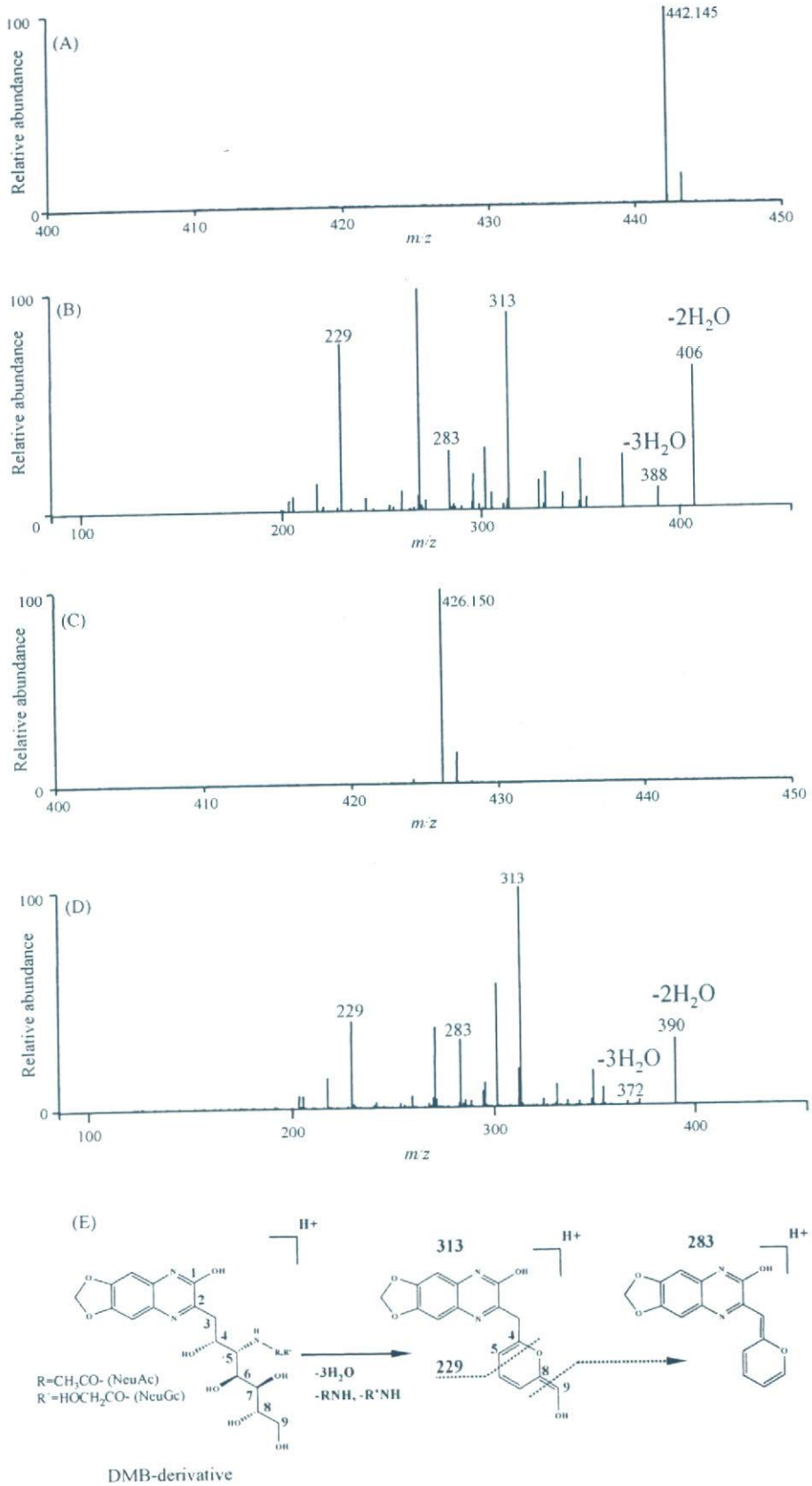

Fig. 2. (A) Typical MS spectrum of peak a. (B) MS/MS spectrum of $[M+H]^+$ (*m/z* 442.145) acquired from around peak a. (C) Typical MS spectrum of peak b. (D) MS/MS spectrum of $[M+H]^+$ (*m/z* 426.150) acquired from around peak b. (E) Fragmentation of DMB-NeuGc and DMB-NeuAc.

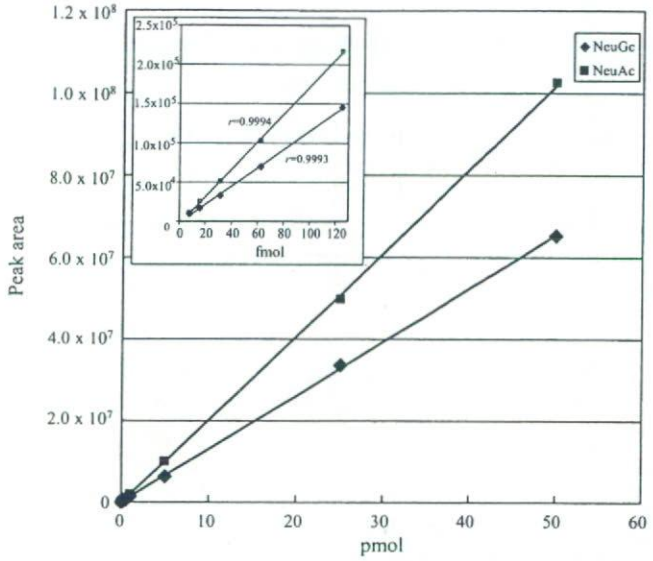

Fig. 3. Calibration curves of DMB-NeuGc ($r = 0.9998$) and DMB-NeuAc ($r = 0.9995$).

tonitrile (pump A) and 0.1% formic acid/80% acetonitrile (pump B) with a linear gradient of 10–90% of B in 30 min at a flow rate of 750 nl/min. On-line MS and MS/MS were performed using an Fourier transformation ion cyclotron resonance (FT)/ion trap (IT) type mass spectrometer (LTQ-FT, Thermo-Electron, San Jose, CA, USA) equipped with a nanoelectrospray ion source (AMR, Tokyo, Japan). DMB-NeuAc and DMB-NeuGc were determined by selected ion monitoring (SIM) in the positive ion mode. The analytical conditions were set to 200 °C for capillary temperature, 1800 eV spray voltage, *m/z* 400–450 scan range, and 35% collision energy. The automatic gain control (AGC) value, which is adjusted for the amount of imported ions for FTMS, was set to 5×10^4. Maximum injection times, which are the adjusted times of imported ions, for ITMS and FTMS, were set to 50 and 1250 ms, respectively.

2.6. Method validation

The linearity of the signal intensity peak area of DMB-NeuAc and DMB-NeuGc was assessed by injections of 0.0078–500 pmol DMB derivatives. Correlation coefficients were calibrated using a least-squares linear regression model. The detection limit (DL) and the quantification limit (QL) were calculated using the formulas $DL = 3.3 \times \sigma/\text{slope}$ (σ: average of noise on chromatograph) and $QL = 10 \times \sigma/\text{slope}$, respectively. Accuracy and precision were determined by measuring three samples, where NeuGc spiked at the concentration of 50 fmol to the membrane fraction of cells cultured in serum-free medium which contains no NeuGc before the derivatization of NeuGc with DMB. Accuracy was calculated by comparison of the mean peak area and the calibration curve. Precision was estimated by relative standard deviation (RSD) from three samples.

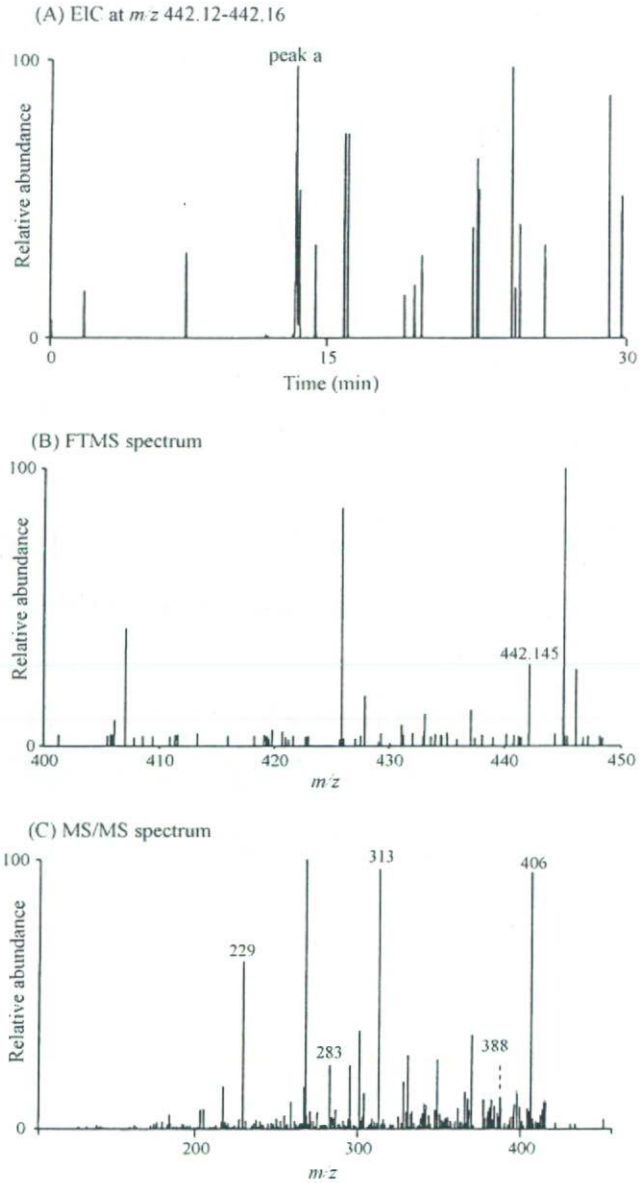

Fig. 4. Detection of DMB-NeuGc in the membrane fractions of HL-60RG cells (2.5×10^3) cultured with 10% FCS. (A) EIC at *m/z* 442.12–442.16 obtained by SIM. (B) Typical MS spectrum of peak a. (C) MS/MS spectrum of $[M+H]^+$ (*m/z* 442.145) acquired from around peak a.

3. Results and discussion

3.1. Analysis of NeuGc and NeuAc by nanoLC/FTMS

It was reported that DMB-NeuGc yielded its dehydrated ion (*m/z* 424) together with molecular ion (*m/z* 442) by MS in the positive ion mode [18,21]. To control the dehydration of molecular ion in the ion trap device, AGC value, which regulates the amount of ions trapped into ion trap device, was set to 5×10^4 (default value, 5×10^5). This value was also useful for the detection of molecular ion of DMB-NeuAc.

Using the AGC value at 5×10^4, SIM (*m/z* 400–450) was carried out in the positive ion mode. When a mix-

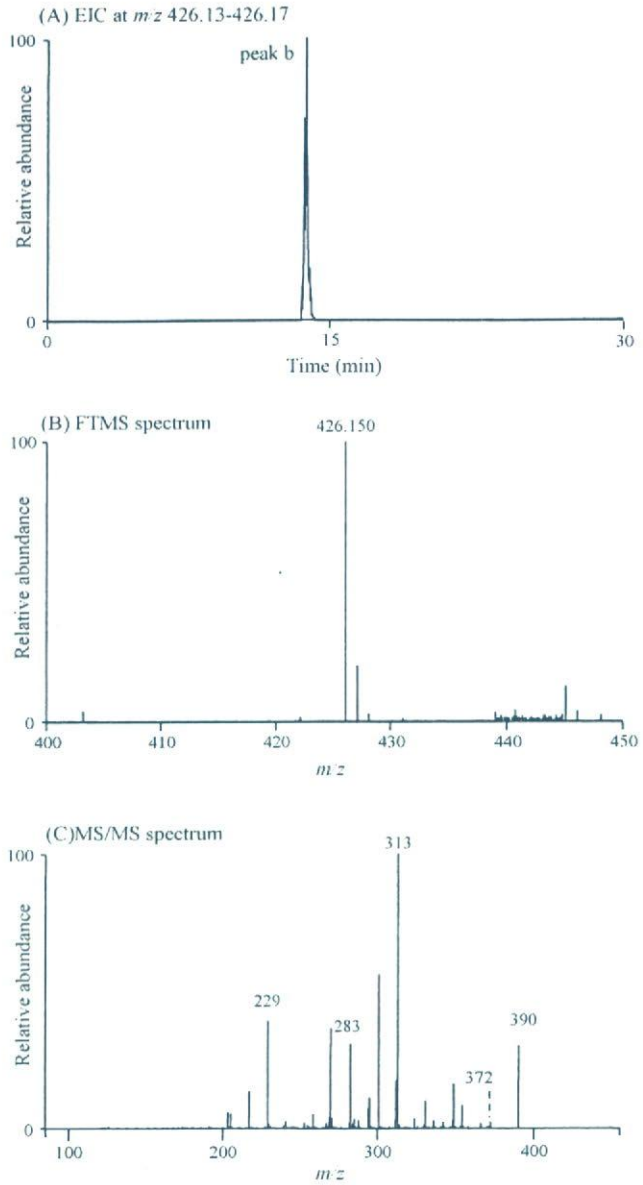

Fig. 5. Detection of DMB-NeuAc in the membrane fractions of HL-60RG cells (2.5×10^3) cultured with 10% FCS. (A) EIC at *m/z* 426.13–426.17 obtained by SIM. (B) Typical MS spectrum of peak b, (C) MS/MS spectrum of $[M+H]^+$ (*m/z* 426.150) acquired from around peak b.

ture of DMB-NeuGc and DMB-NeuAc (2 pmol each) was subjected to nanoLC/MS, two peaks appeared at 14 min (peak a) and 15 min (peak b) on the extracted ion chromatogram (EIC) at *m/z* 426.13–426.17 and *m/z* 442.12–442.16 (Fig. 1).

As shown in Fig. 2A, the *m/z* values of molecular ions around 14 min (*m/z* 442.145) suggest the elution of DMB-NeuGc in peak a. The structure of the DMB derivative at peak a was confirmed by the product ion spectra acquired from $[M+H]^+$ (*m/z* 442.145) as a precursor ion (Fig. 2B). Product ions missing two and three molecules of H_2O were found at *m/z* 406 and 388 in MS/MS spectra. Ions losing three H_2O and glycolyl groups (*m/z* 313), cross-ring fragment ion (*m/z* 229) and fragment ion yielded by loss of formaldehyde (*m/z* 283) were also formed by

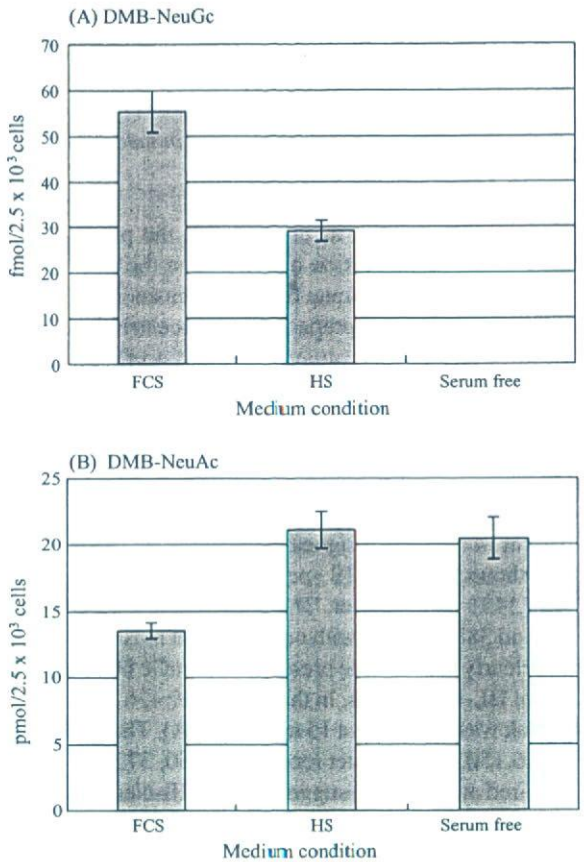

Fig. 6. Levels of (A) NeuGc and (B) NeuAc in the membrane fraction of HL-60RG cells (2.5×10^3) cultured with 10% FCS, 10% human serum (HS) and serum-free medium. Values are the means ± SD ($n = 3$).

MS/MS (Fig. 2E). The fragment pattern of the MS/MS spectrum from $[M+H]^+$ (*m/z* 442.145) was consistent with that of DMB-NeuGc in the previous report [21]. Fragments at *m/z* 406 and 388 are DMB-NeuGc characteristic ions, which could be used for specific determination of DMB-NeuGc. Likewise, peak b was identified as DMB-NeuAc by molecular ions (*m/z* 426.150) and their product ions (*m/z* 390, 372, 313, 283 and 229) formed by MS/MS of $[M+H]^+$ (*m/z* 426.150) as a precursor ion (Fig. 2C and D).

Calibration curves were prepared by the injection of DMB-NeuGc and DMB-NeuAc from 0.0078 to 500 pmol. The linearity of DMB-NeuGc and DMB-NeuAc was confirmed in the range of 0.0078–50 pmol with the regression equations of $Y = 1.31 \times 10^6 X - 9028.5$ ($r = 0.9998$) and $Y = 2.03 \times 10^6 X - 21548.0$ ($r = 0.9995$), respectively (Fig. 3). DL and QL of DMB-NeuGc were 8.6 and 26.3 fmol, and those of DMB-NeuAc were 5.6 and 16.9 fmol, respectively. The use of FT/MS gave an accuracy of 92.4% by eliminating contaminants by using accurate *m/z* values. The precision of this method for NeuGc was 7.3%. Compared to the former method, in which a micro or semi-micro column and the quadrupole mass spectrometer were used for the detection of picomole levels of DMB derivatives, SIM by using nanoLC/FTMS achieved the specific detection of DMB-derivatized sialic acids at a lower level. The method using nanoLC/FTMS and nanoLC/MS/MS allows not

only the determination of DMB-derivatives with similar sensitivity as the fluorescence detection but also the identification of sialic acid species.

3.2. Quantification of NeuAc and NeuGc in membrane fraction of HL-60RG cells

Using HL-60RG cells as model cells, the potential of this method for the quantification of NeuGc on the cell membrane was evaluated. The membrane fraction from cells (1×10^6) cultured with 10% FCS was prepared by ultracentrifugation. Sialic acids were released by treatment with 2 M acetic acid at 80 °C for 3 h and derivatized with DMB. DMB derivatives (2.5×10^3 cells) were subjected to nanoLC/MS and nanoLC/MS/MS in SIM mode. As shown in Fig. 4A, some peaks appeared in EIC at *m/z* 442.12–442.16. Based on the retention time as well as the *m/z* value of molecular ion (*m/z* 442.145), peak a that appeared at 14 min was assigned to be a peak of NeuGc (Fig. 4B). Fig. 4C shows the MS/MS spectrum acquired from $[M+H]^+$ (*m/z* 442.145) as precursor. The NeuGc-characteristic ions at *m/z* 406 and 388 together with other product ions at *m/z* 313, 283 and 229 clearly indicate the presence of NeuGc in the membrane fraction of HL-60RG cells. In the EIC at *m/z* 426.13–426.17, the single peak was observed at 15 min (Fig. 5A). The molecular ion at *m/z* 426.150, and product ions at *m/z* 390, 372, 313, 283 and 229 acquired at 15.13 min suggest that DMB-NeuAc is eluted in peak b (Fig. 5B and C). The levels of NeuGc and NeuAc in the membrane fraction from HL-60RG cells (2.5×10^3 cells) cultured with 10% FCS were 55.4 ± 4.6 fmol and 13.5 ± 0.6 pmol, respectively (Fig. 6)

After the cultivation of HL-60RG cells with human serum for 10 days (medium was changed four times), NeuGc and NeuAc were determined by the proposed method. Fig. 7A shows the EIC at *m/z* 442.12–442.16 obtained by nanoLC/MS. In spite of cultivation in human serum, an obvious peak still appeared at 14 min. Molecular ion (*m/z* 442.145) and NeuGc-characteristic product ions found in the MS/MS spectrum acquired from the molecular ion clearly indicate the presence of NeuGc in the membrane fraction (Fig. 7B and C). The levels of NeuGc and NeuAc in cells (2.5×10^3) cultured in 10% human serum were 29.2 ± 2.4 fmol and 21.0 ± 1.4 pmol, respectively (Fig. 6).

In contrast, no significant peaks appeared in EIC at *m/z* 442.12–442.16 when HL-60RG cells were cultured in serum-free medium for 14 days (medium was changed four times). The level of NeuAc in cells cultured in serum-free medium was 20.5 ± 1.6 pmol (Fig. 6).

As shown in Figs. 4A and 7A, there are many different molecules detected at *m/z* 442.14–442.16 in the cells, which makes it difficult to determine a small amount of NeuGc in the membrane fraction by the low-resolution mass spectrometry. The DMB-NeuGc-specific detection was achieved by acquisition of both the accurate mass by FTMS and the characteristic product ions arisen from DMB-NeuGc by MS/MS.

Our method needs only 2.5×10^3 cells for one injection and is applicable to the determination of NeuGc in cell therapy products. The incorporation of dietary NeuGc into human

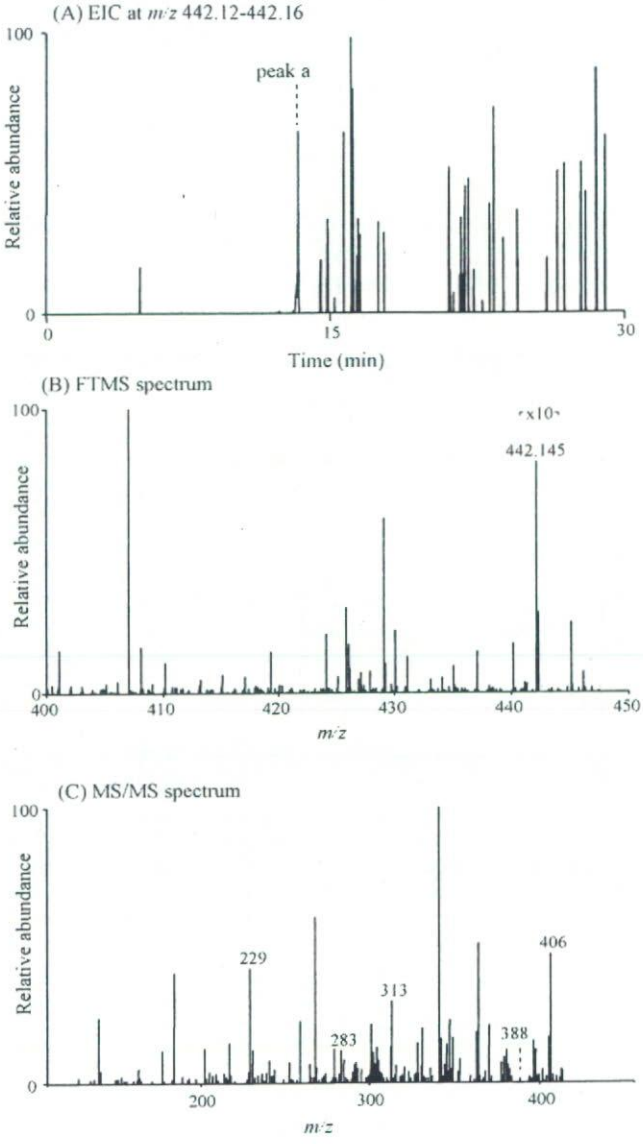

Fig. 7. Detection of DMB-NeuGc in the membrane fractions of HL-60RG cells (2.5×10^3) cultured with 10% human serum. (A) EIC at *m/z* 442.12–442.16 obtained by SIM. (B) Typical MS spectrum of peak a. (C) MS/MS spectrum of $[M+H]^+$ (*m/z* 442.145) acquired from around peak a.

serum has been reported by Tangvoranuntalul et al. [23], which has raised concerns about NeuGc contamination of cell therapy products through cultivation with human serum. Although using our method, we demonstrated the existence of NeuGc in human cells cultured with human serum, NeuGc could not be detected in human cells cultured in serum-free medium in which no NeuGc exists. These results suggest the difficulty of avoiding NeuGc contamination of cell therapy products during the manufacturing process. Further study to assess the immunogenicity of incorporated NeuGc is necessary to ensure the safety and efficacy of cell therapy products, and our method is useful for the sensitive and quantitative analysis of NeuGc in cell therapy products.

Acknowledgements

This study was supported in part by a Grant-in-Aid from the Ministry of Health Labor and Welfare, and Core Research for the Evolutional Science and Technology Program, Japan Science and Technology Corp.

References

[1] C. Traving, R. Schauer, Cell Mol. Life Sci. 54 (1998) 1330.
[2] T. Angata, A. Varki, Chem. Rev. 102 (2002) 439.
[3] A. Varki, Glycobiology 2 (1992) 25.
[4] R. Schauer, Adv. Carbohydr. Chem. Biochem. 40 (1982) 131.
[5] S. Kitazume, K. Kitajima, S. Inoue, S.M. Haslam, H.R. Morris, A. Dell, W.J. Lennarz, Y. Inoue, J. Biol. Chem. 271 (1996) 6694.
[6] R. Schauer, J. Haverkamp, M. Wember, J.P. Kamerling, J.F. Vliegenthart, Eur. J. Biochem. 62 (1976) 237.
[7] N. Kawasaki, S. Itoh, M. Ohta, T. Hayakawa, Anal. Biochem. 316 (2003) 15.
[8] M. Nakano, K. Kakehi, M.H. Tsai, Y.C. Lee, Glycobiology 14 (2004) 431.
[9] E.A. Muchmore, S. Diaz, A. Varki, Am. J. Phys. Anthropol. 107 (1998) 187.
[10] A. Irie, S. Koyama, Y. Kozutsumi, T. Kawasaki, A. Suzuki, J. Biol. Chem. 273 (1998) 15866.
[11] H.H. Chou, H. Takematsu, S. Diaz, J. Iber, E. Nickerson, K.L. Wright, E.A. Muchmore, D.L. Nelson, S.T. Warren, A. Varki, Proc. Natl. Acad. Sci. U. S. A. 95 (1998) 11751.
[12] H. Higashi, M. Naiki, S. Matuo, K. Okouchi, Biochem. Biophys. Res. Commun. 79 (1977) 388.
[13] J.M. Merrick, K. Zadarlik, F. Milgrom, Int. Arch. Allergy Appl. Immunol. 57 (1978) 477.
[14] M.J. Martin, A. Muotri, F. Gage, A. Varki, Nat. Med. 11 (2005) 228.
[15] A. Heiskanen, T. Satomaa, S. Tiitinen, A. Laitinen, S. Mannelin, U. Impola, M. Mikkola, C. Olsson, H. Miller-Podraza, M. Blomqvist, A. Olonen, H. Salo, P. Lehenkari, T. Tuuri, T. Otonkoski, J. Natunen, J. Saarinen, J. Laine, Stem Cells 25 (2007) 197.
[16] A.E. Manzi, S. Diaz, A. Varki, Anal. Biochem. 188 (1990) 20.
[17] S. Hara, M. Yamaguchi, Y. Takemori, K. Furuhata, H. Ogura, M. Nakamura, Anal. Biochem. 179 (1989) 162.
[18] M. Bardor, D.H. Nguyen, S. Diaz, A. Varki, J. Biol. Chem. 280 (2005) 4228.
[19] M. Ito, K. Ikeda, Y. Suzuki, K. Tanaka, M. Saito, Anal. Biochem. 300 (2002) 260.
[20] F.N. Lamari, N.K. Karamanos, J. Chromatogr. B 781 (2002) 3.
[21] A. Klein, S. Diaz, I. Ferreira, G. Lamblin, P. Roussel, A.E. Manzi, Glycobiology 7 (1997) 421.
[22] H.H. Chou, T. Hayakawa, S. Diaz, M. Krings, E. Indriati, M. Leakey, S. Paabo, Y. Satta, N. Takahata, A. Varki, Proc. Natl. Acad. Sci. U. S. A. 99 (2002) 11736.
[23] P. Tangvoranuntakul, P. Gagneux, S. Diaz, M. Bardor, N. Varki, A. Varki, E. Muchmore, Proc. Natl. Acad. Sci. U. S. A. 100 (2003) 12045.

Fiber-Modified Adenovirus Vectors Decrease Liver Toxicity through Reduced IL-6 Production[1]

Naoya Koizumi,*† Tomoko Yamaguchi,* Kenji Kawabata,* Fuminori Sakurai,* Tomomi Sasaki,* Yoshiteru Watanabe,† Takao Hayakawa,‡ and Hiroyuki Mizuguchi[2]*§

Adenovirus (Ad) vectors are one of the most commonly used viral vectors in gene therapy clinical trials. However, they elicit a robust innate immune response and inflammatory responses. Improvement of the therapeutic index of Ad vector gene therapy requires elucidation of the mechanism of Ad vector-induced inflammation and cytokine/chemokine production as well as development of the safer vector. In the present study, we found that the fiber-modified Ad vector containing poly-lysine peptides in the fiber knob showed much lower serum IL-6 and aspartate aminotransferase levels (as a maker of liver toxicity) than the conventional Ad vector after i.v. administration, although the modified Ad vector showed higher transgene production in the liver than the conventional Ad vector. RT-PCR analysis showed that spleen, not liver, is the major site of cytokine, chemokine, and IFN expression. Splenic CD11c$^+$ cells were found to secret cytokines. The tissue distribution of Ad vector DNA showed that spleen distribution was much reduced in this modified Ad vector, reflecting reduced IL-6 levels in serum. Liver toxicity by the conventional Ad vector was reduced by anti-IL-6R Ab, suggesting that IL-6 signaling is involved in liver toxicity and that decreased liver toxicity of the modified Ad vector was due in part to the reduced IL-6 production. This study contributes to an understanding of the biological mechanism in innate immune host responses and liver toxicity toward systemically administered Ad vectors and will help in designing safer gene therapy methods that can reduce robust innate immunity and inflammatory responses. ***The Journal of Immunology,*** **2007, 178: 1767–1773.**

Recombinant adenovirus (Ad)[3] vectors are widely used for gene therapy experiments and clinical gene therapy trials. One of the limitations of Ad vector-mediated gene transfer is the immune response after systemic administration of the Ad vector (1, 2). The immune response to the Ad vector and Ad vector-transduced cells dramatically affects the kinetics of the Ad vector-delivered genes and the gene products. The potent immunogenic toxicities and consequent short-lived transgene expression of Ad vectors are undesirable properties if Ad vectors are to be more broadly applied. The immunogenic toxicities associated with the use of Ad vectors involve both innate and adaptive immune responses.

In the first generation Ad vector lacking the *E1* gene, leaky expression of viral genes from the vector stimulates an immune response against the Ad vector-transduced cells (3–5). The CTL response can be elicited against viral gene products and/or transgene products expressed by transduced cells. The molecular mechanism of this toxicity has been studied extensively, and the helper-dependent (gutted) Ad vector, which deletes all of the viral protein-coding sequences, has been developed to overcome this limitation (6–8). The humoral virus-neutralizing Ab responses against the Ad capsid itself are another limitation, preventing transgene expression upon the subsequent administration of vectors of the same serotype. Because hexons are mainly targeted by neutralizing Abs, hexon modification has been reported to allow for escape from neutralizing Abs (9). The Ad vectors belonging to types of the subgroup other than Ad type 5, including an Ad type 11- or 35-based vector, or to species other than human have also been developed (10–13).

Regarding the innate immune response, shortly after systemic injection of the Ad vector cytokines/chemokines are produced and an inflammatory response occurs in response to the Ad vector and Ad vector-transduced cells. It has been reported that activated Kupffer cells (and monocytes and resident macrophages) and dendritic cells (DC) release proinflammatory cytokines/chemokines such as IL-6, TNF-α, IP-10, and RANTES, causing the activation of an innate immune response (14, 15). NF-κB activation is likely to play a central role in inflammatory cytokine/chemokine production (16, 17). Although many papers regarding the innate immune response to the Ad vector have been published thus far, the biological mechanism has not been clearly elucidated. Even the cell types responsible for the innate immune response have not been identified. Understanding the mechanism of and identifying the cell types responsible for the innate immune response and liver inflammation are crucial to the construction of new vectors that are safer and efficiently transduce target tissue. Modification of the Ad vector with polyethylene glycol (PEG) reduces the innate immune response and also prolongs persistence in the blood and circumvents neutralization of the Ad vectors by Abs (18–21). We have previously reported that the mutant Ad vector ablating coxsackievirus and Ad receptor (CAR) (the first receptor) binding, α_v integrin (the secondary receptor) binding, and heparan sulfate glycosaminoglycan (HSG) (the third receptor) binding reduced (or blunted)

*Laboratory of Gene Transfer and Regulation, National Institute of Biomedical Innovation, Osaka, Japan; †Department of Pharmaceutics and Biopharmaceutics, Showa Pharmaceutical University, Tokyo, Japan; ‡Pharmaceuticals and Medical Devices Agency, Tokyo, Japan; and §Graduate School of Pharmaceutical Sciences, Osaka University, Osaka, Japan

Received for publication August 29, 2006. Accepted for publication November 10, 2006.

The costs of publication of this article were defrayed in part by the payment of page charges. This article must therefore be hereby marked *advertisement* in accordance with 18 U.S.C. Section 1734 solely to indicate this fact.

[1] This work was supported by grants from the Ministry of Health, Labor, and Welfare of Japan.

[2] Address correspondence and reprint requests to Dr. Hiroyuki Mizuguchi, Laboratory of Gene Transfer and Regulation, National Institute of Biomedical Innovation, Asagi 7-6-8, Saito, Ibaraki, Osaka 567-0085, Japan. E-mail address: mizuguch@nibio.go.jp

[3] Abbreviations used in this paper: Ad, adenovirus; AST, aspartate aminotransferase; CAR, coxsackievirus and Ad receptor; DC, dendritic cell; HSG, heparan sulfate glycosaminoglycan; PEG, polyethylene glycol; VP, virus particle.

liver toxicity and IL-6 production (22). However, these two Ad vectors mediate significantly lower tissue transduction due to steric hindrance by PEG chains and a loss of binding activity to the receptor, respectively (20–22). An Ad vector showing efficient transduction and reduced innate immune response has not yet been developed.

In the present study, we elucidate the molecular mechanism of the innate immune response by the Ad vector and characterize the safer Ad vector, which reduces the innate immune response and liver toxicity. We found that the fiber-modified Ad vector containing a stretch of lysine residues (K7 (KKKKKKK) peptide) (23–25) that target heparan sulfates on the cellular surface greatly reduced IL-6 and liver toxicity after i.v. injection into mice compared with the conventional Ad vector. IL-6 and the other immune cytokines, chemokines, and IFNs were mainly produced from the spleen and especially from conventional DC ($CD11c^+B220^-$ cells), not the liver. The spleen distribution of the K7-modified Ad vector was reduced compared with the conventional Ad vector. The K7-modified Ad vector decreased the liver toxicity (aspartate aminotransferase (AST) levels), at least in part due to the reduced serum IL-6 levels. Importantly, this K7-modified Ad vector maintained high transduction efficiency in vivo and showed somewhat higher transgene production in the liver than a conventional Ad vector.

Materials and Methods

Ad vector

Two luciferase-expressing Ad vectors, Ad-L2 and AdK7-L2, have been constructed previously (25, 26). The CMV promoter-driven luciferase gene derived from the pGL3-Control was inserted into the E1 deletion region of the Ad genome. Ad-L2 contains wild-type fiber, whereas AdK7-L2 contains the polylysine peptide KKKKKKK in the C-terminal of the fiber knob (25). Viruses (Ad-L2 and AdK7-L2) were prepared as described previously (25) and purified by $CsCl_2$ step gradient ultracentrifugation. Determination of virus particle titers was accomplished spectrophotometrically by the method of Maizel et al. (27).

Ad-mediated transduction in vivo

Ad-L2 or AdK7-L2 were i.v. administered to C57BL6 mice (1.0×10^{10} virus particles (VP)) (6-wk-old males obtained from Nippon SLC). Forty-eight hours later, the heart, lung, liver, kidney, and spleen were isolated and homogenated as previously described (28). Luciferase production was determined using a luciferase assay system (PicaGene 5500; Toyo Inki). Protein content was measured with a Bio-Rad assay kit using BSA as a standard.

The amounts of Ad genomic DNA in the each organ were quantified with the TaqMan fluorogenic detection system (ABI Prism 7700 sequence detector; PerkinElmer Applied Biosystems). Samples were prepared with DNA templates isolated from each organ (25 ng) by an automatic nucleic acid isolation system (NA-2000; Kurabo Industries). The amounts of Ad DNA were quantified with the TaqMan fluorogenic detection system (PerkinElmer Applied Biosystems) as described in our previous report (22).

To analyze the involvement of IL-6 signaling in liver toxicity in response to Ad vector administration, 100 μg per mouse of an anti-IL-6R Ab (clone D7715A7; BioLegend) that specifically blocks IL-6 signaling was i.p. administered to C57BL6 mice 1.5 h before Ad-L2 administration (3.0×10^{10} VP). Rabbit IgG (clone R3-34; BD Biosciences) was administered as a control. Serum samples and liver tissue were collected 48 h later, and AST levels in the serum and luciferase production in the liver were determined.

Liver serum enzymes and cytokine levels after systemic administration

Blood samples were collected by the inferior vena cave at the indicated times (3 or 48 h) after i.v. administration of Ad-L2 or AdK7-L2 (3.0×10^{10} and 1.0×10^{11} VP, respectively). IL-6 and IL-12 levels in serum samples collected at 3 h after Ad injection were measured by an ELISA kit (BioSource International). The levels of AST in serum samples collected at 24 and 48 h were measured with the Transaminase-CII kit (Wako Pure Chemical). Forty-eight hours after the Ad vector injection, the mice were killed and their livers were collected. The liver was washed, fixed in 10% formalin, and embedded in paraffin. After sectioning, the tissue was dewaxed in ethanol, rehydrated, and stained with H&E. This process was commissioned to the Applied Medical Research Laboratory (Osaka, Japan).

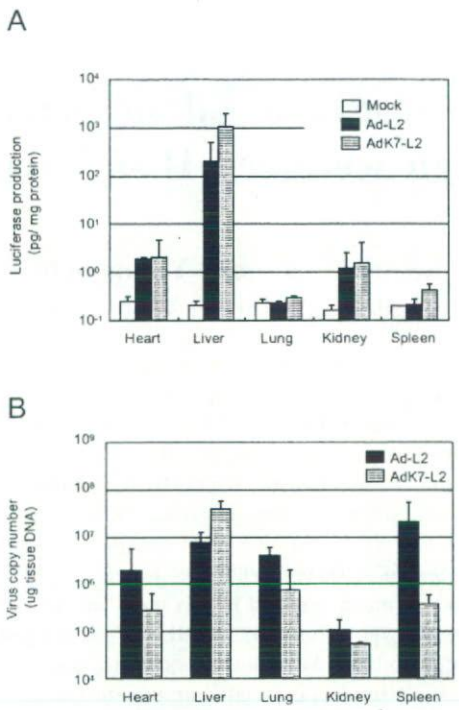

FIGURE 1. Luciferase production and biodistribution of viral DNA after the i.v. administration of Ad-L2 or AdK7-L2 into mice. Ad-L2 or AdK7-L2 (1.0×10^{10} VP) was i.v. injected into the mice. Forty-eight hours later, the heart, lung, liver, kidney, and spleen were harvested, and luciferase production (*A*) and Ad vector DNA (*B*) in each organ were measured by a luciferase assay system or the quantitative TaqMan PCR assay, respectively. All data represent the means ± SD of 4–6 mice.

Cytokines and chemokines mRNA levels in tissue after systemic administration

Total tissue RNA samples were isolated by the reagent ISOGEN (Wako Pure Chemical) 3 h after the i.v. administration of Ad-L2 or AdK7-L2 (1.0×10^{11} VP). Reverse transcription was performed using the SuperScript first-strand synthesis system for first-strand cDNA synthesis (Invitrogen Life Technologies) according to the instructions of the manufacturer. IL-6 and IL-12 mRNA in the liver and spleen were quantified with the TaqMan fluorogenic detection system (PerkinElmer Applied Biosystems). Semiquantified RT-PCR analysis was also performed to determine mRNA levels of the cytokines, chemokines, and IFNs (total eight mRNA). The primer sequences and probes were as follows: IL-6 forward, 5′-GAG GAT ACC ACT CCC AAC AGA CC-3′; IL-6 reverse, 5′-AAG TGC ATC ATC GTT GTT CAT ACA-3′ (reverse); IL-6 probe, 5′-CAG AAT TGC CAT TGC ACA ACT CTT TTC TCA-3′; IL-12p40 forward, 5′-GGA AGC ACG GCA GCA GAA TA-3′; IL-12p40 reverse, 5′-AAC TTG AGG GAG AAG TAG GAA TGG-3′; IL-12p40 probe, 5′-CAT CAT CAA ACC AGA CCC GCC CAA-3′; TNF-α forward, 5′-CCT GTA GCC CAC GTC GTA GC-3′; TNF-α reverse, 5′-TTG ACC TCA GCG CTG AGT TG-3′; RANTES forward, 5′-ATG AAG ATC TCT GCA GCT GCC CTC ACC-3′; RANTES reverse, 5′-CTA GCT CAT CTC CAA ATA GTT GAT G-3′; MIP-2 forward, 5′-ACC TGC CGG CTC CTC AGT GCT GC-3′; MIP-2 reverse, 5′-GGC TTC AGG GTC AAG GCA AAC-3′; IFN-α forward, 5′-AGG CTC AAG CCA TCC CTG T-3′; IFN-α reverse, 5′-AGG CAC AGG GGC TGT CTT TCT TCT-3′; IFN-β forward, 5′-TTC CTG CTG TGC TTC TCC AC-3′; IFN-β reverse, 5′-GAT TCA CTA CCA GTC CCA GAG TC-3′; IFN-γ forward, 5′-GAG GAT ACC ACT CCC AAC AGA CC-3′; IFN-γ reverse, 5′-AAG TGC ATC ATC GTT GTT CAT ACA-3′; GAPDH forward, 5′-TTC ACC ACC ATG GAG AAG GC-3′; and GAPDH reverse, 5′-GGC ATG GAC TGT GGT CAT GA-3′. The expected sizes of the PCR products are as follows: IL-6, 193 bp; IL-12p40, 155 bp; TNF-α, 374 bp; RANTES, 252 bp; MIP-2, 221 bp; IFNα, 272 bp; IFNβ, 607 bp; IFN-γ, 306 bp; and GAPDH, 237 bp.

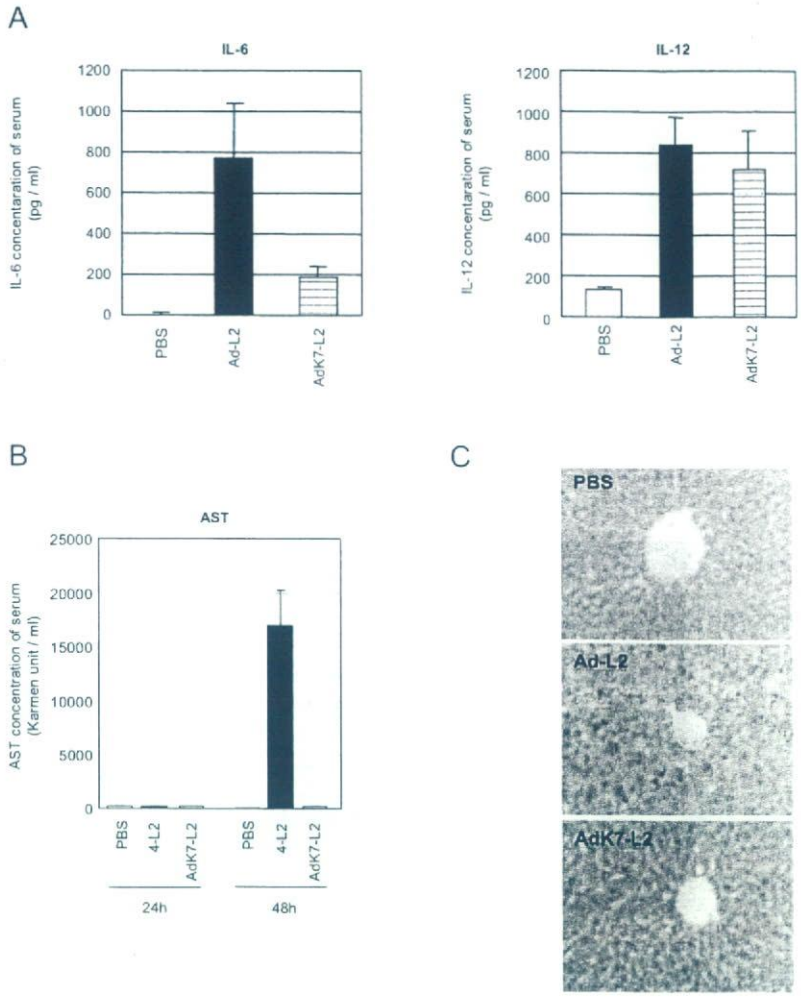

FIGURE 2. Cytokines and liver enzyme levels in serum after the systemic administration of Ad-L2 or AdK7-L2 into mice. Blood samples were collected by inferior vena cave at 3 h (*A*) or 24 and 48 h (*B*) after i.v. administration of Ad-L2 or AdK7-L2 (1.0×10^{11} VP for *A* or 3.0×10^{10} VP for *B*). The livers were collected after 48 h following the injection (3.0×10^{10} VP) (*C*). *A*, IL-6 and IL-12 levels in the serum were measured by ELISA. *B*, AST levels in the serum were measured using a Transaminase-CII kit. *C*, Paraffin sections of the livers were prepared. Each section was stained with H&E. Data represent the means ± SD of four mice.

Cell sorting of splenic cells

Splenic conventional DC, plasmacytoid DC, and B cells, which were $CD11c^+B220^-$, $CD11c^+B220^+$, and $CD11c^-B220^+$ cells, respectively, were sorted by FACS Aria (BD Biosciences). Total RNA samples were isolated from each cell by the reagent ISOGEN, and RT-PCR analysis was then performed as described above.

Results

This study was undertaken to elucidate the biological mechanism in the innate immune host responses toward i.v. administered Ad vector. The relationship between the innate immune response and liver toxicity by systemic administration of the Ad vectors was also examined.

Gene transduction and Ad vector accumulation in vivo

In this study we used the conventional Ad vector (Ad-L2) and a fiber-modified Ad vector containing a polylysine (K7) peptide (AdK7-L2), both of which express luciferase under the control of the CMV promoter. First, we examined luciferase production in the organ and the biodistribution of viral DNA after i.v. administration of AdK7-L2 (1.0×10^{10} VP) into mice compared with Ad-L2 (see Fig. 3). The vector dose of 1.0×10^{10} VP was selected because this dose did not induce any apparent toxicity (IL-6 and AST production) with either Ad-L2 or AdK7-L2. When a higher dose (3.0×10^{10} or 1.0×10^{11} VP) was used, only Ad-L2 and not AdK7-L2 showed toxicity (described later), which does not reflect an exact comparison of the transduction efficiency. The Ad type 5-based vector delivers the foreign gene predominantly in the liver after i.v. injection into mice (29, 30). Interestingly, AdK7-L2 mediated ~6-fold higher liver transduction than Ad-L2 (Fig. 1*A*). In contrast, the luciferase production in the heart, lung, kidney, and spleen in response to AdK7-L2 was similar to that in response to Ad-L2. To examine the biodistribution of Ad-L2 and AdK7-L2 in mice, the amounts of Ad DNA in each organ 48 h after the injection of Ad vectors were measured with the TaqMan fluorogenic detection system. More AdK7-L2 DNA accumulated in the liver than Ad-L2 DNA (Fig. 1*B*), although the amounts of AdK7-L2 DNA in the heart, lung, kidney, and spleen were less than those of Ad-L2 DNA. In particular, the amounts of AdK7-L2 DNA in the spleen were ~56-fold less than those of Ad-L2 DNA. The data regarding luciferase production (Fig. 1*A*) and the amounts of Ad DNA in most organs (Fig. 1*B*) showed discrepancies. Luciferase production in the liver was >2 log order higher than that in other organs, while the amounts of Ad DNA in liver were not as striking among the organs compared with luciferase production. This difference is likely due to the difference in the amount of nonspecific viral uptake among the organs. Reduced spleen accumulation of AdK7-L2 DNA, compared with Ad-L2 DNA, was also observed at a dose of 1.0×10^{11} VP (data not shown).

Serum cytokines and AST levels

The systemic administration of Ad vectors results in the initiation of strong innate immune responses and inflammation in animals and humans (1), and this toxicity limits the utility of Ad vectors for gene therapy. To evaluate the innate immune response and liver toxicity of each Ad vector, we measured the levels of IL-6, IL-12, and AST in serum. Because IL-6 in the serum and hepatic toxicity

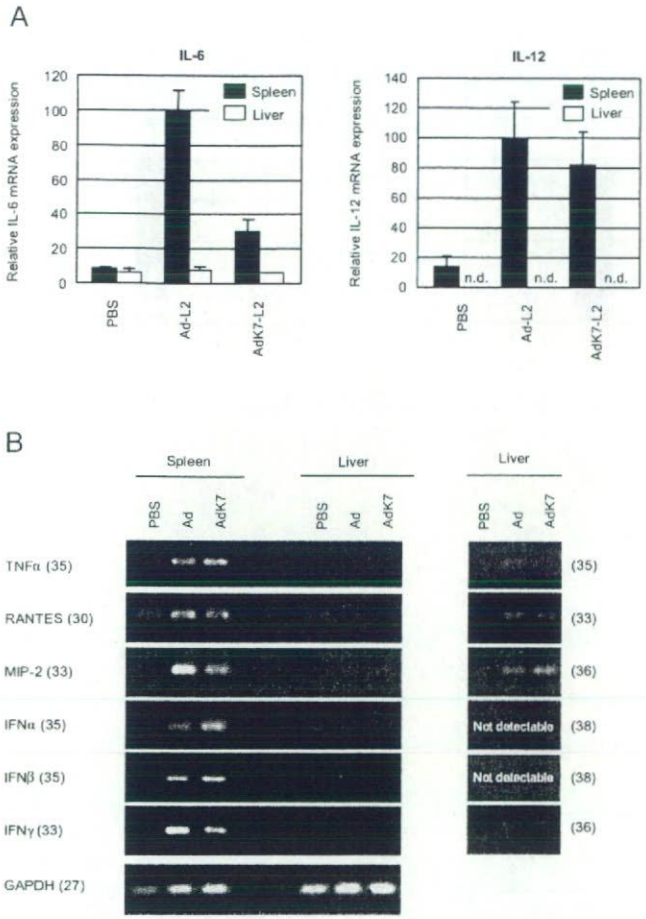

FIGURE 3. Cytokine, chemokine, and IFN mRNA levels in liver and spleen after the systemic administration of Ad-L2 or AdK7-L2 into mice. Total mRNA samples were isolated from liver and spleen at 3 h after i.v. administration of Ad-L2 or AdK7-L2 (1.0×10^{11} VP). After the reverse transcriptase reaction, IL-6 and IL-12 cDNA were measured with the quantitative TaqMan PCR assay (*A*). The expression of TNF-α, RANTES, MIP-2, IFN-α, IFN-β, and IFN-γ was measured by semiquantitative RT-PCR assay (*B*). All data represent the means ± SD of four mice. Cycle number is given in parentheses.

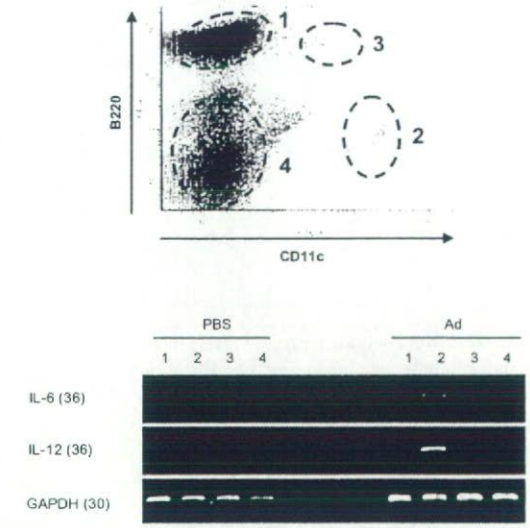

FIGURE 4. IL-6 and IL-12 mRNA levels in splenic CD11c-positive cells after the systemic administration of Ad-L2 into mice. Total mRNA samples were isolated from sorted splenic cells 3 h after i.v. administration of Ad-L2 (1.0×10^{11} VP). The expression levels of IL-6 and IL-12 mRNA were measured by RT-PCR assay. *Lane 1*, B cell ($B220^+CD11c^-$); *lane 2*, conventional DC ($B220^-CD11c^+$); *lane 3*, plasmacytoid DC ($B220^+CD11c^+$); *lane 4*, other cells ($B220^-CD11c^-$). Cycle number is given in parentheses.

analysis was detected at a dose of $>1.0 \times 10^{11}$ or 3.0×10^{10} VP, respectively, these doses were used.

IL-6 levels in response to AdK7-L2 were one-fourth of those with Ad-L2 (Fig. 2*A*). In contrast, there was no difference in serum IL-12 levels between Ad-L2 and AdK7-L2. Thus, IL-6 and IL-12 appear to be produced by a different mechanism. TNF-α in the serum after the injection of Ad-L2 or AdK7-L2 could not be detected (data not shown). Ad-L2 led to high levels of serum AST at 48 h after injection, while AdK7-L2 did not induce AST (Fig. 2*B*). At 24 h, neither Ad-L2 nor AdK7-L2 induced AST. In histological analysis, degranulation or denucleation occurred in hepatocytes from Ad-L2, while AdK7-L2 did not induce hepatocyte toxicity (Fig. 2*C*). The results using AdK7-L2 were similar to those in the untreated mice (Fig. 2, *B* and *C*), suggesting that AdK7-L2 does not show any liver toxicity. These results suggest that AdK7-L2 shows less IL-6 production and almost no liver toxicity.

Cytokines mRNA levels in liver and spleen cells

Ad vectors induce the expression of various cytokines and chemokines in the innate immune responses by effector cells such as macrophages and DC (15, 17, 31–33). Liver and spleen are two major organs responsible for the location of immune cells. We attempted to determine which organ (liver or spleen) produces cytokines, chemokines, and IFNs (IL-6, IL-12, TNF-α, RANTES, MIP-2, IFNα, IFNβ, and IFN-γ) by quantitative real-time RT-PCR or semiquantitative RT-PCR analysis. IL-6 and IL-12 mRNA levels were not induced in the liver after i.v. administration of Ad vectors (Fig. 3*A*). This result was also checked by the result that specific IL-6 and IL-12 mRNA bands were not detected in the liver by RT-PCR analysis (data not shown). Expression of TNF-α, RANTES, MIP-2, IFN-α, IFN-β, and IFN-γ mRNA was also detected mainly in the spleen, not the liver (Fig. 3*B*). IL-6, MIP-2, and IFN-γ mRNA levels in the spleen in response to AdK7-L2 were lower than those in response to Ad-L2. In the liver, TNF-α, RANTES, MIP-2, and IFN-γ mRNA were detected by a high cycle number of PCR after Ad (Ad-L2 or AdK7-L2) injection, whereas IFN-α and IFN-β could be not detected (Fig. 3*B*).

We next identified the cell types responsible for the IL-6 and IL-12 expression in the spleen after i.v. administration of the Ad vector (Ad-L2). Spleen cells were sorted by FACS Aria based on the expression of CD11c and B220 in conventional DC ($CD11c^+B220^-$), plasmacytoid DC ($CD11c^+B220^+$), and B cells ($CD11c^-B220^+$ cells). IL-6 and IL-12 mRNA were mainly detected in the splenic conventional DC. Only a faint band of IL-12 mRNA was also detected in the splenic plasmacytoid DC ($CD11c^+B220^+$) (Fig. 4). These results suggest that splenic conventional DC are major effector cells of innate immune response (at least IL-6 and IL-12 production) against systemically administered Ad vectors.

Elimination of IL-6 signaling reduces liver toxicity

It has previously been shown that TNF-α is likely to be involved in host responses to Ad vectors in vitro and in vivo (34). Recently, Shayakhmetov et al. (35) have reported that IL-1 signaling, not TNF-α signaling, is involved in Ad vector-associated liver toxicity after i.v. administration. However, the mechanism of liver toxicity

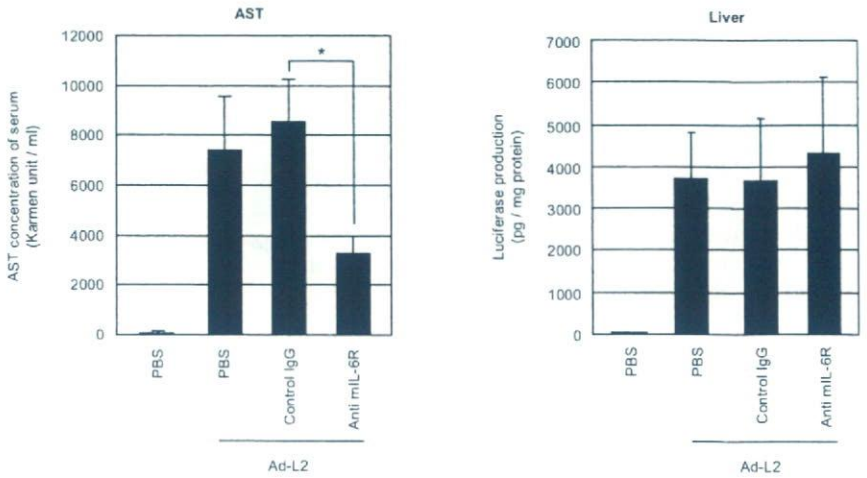

FIGURE 5. Effects of serum IL-6 on serum AST levels and liver luciferase production after the systemic administration of Ad-L2 into mice. C57BL/6 mice were i.p. administered 100 μg per mouse of anti-IL-6R Ab (clone D7715A7), which was specific for blocking IL-6 signaling, or rabbit IgG as a control (clone; R3-34). Ad-L2 or AdK7-L2 (3.0×10^{10} VP) was i.v. injected into the mice 1.5 h later. Blood samples and liver tissue were collected 48 h after the injection of Ad-L2. The AST levels in the serum were measured using a Transaminase-CII kit. Luciferase production in the liver was measured by a luciferase assay system. All data represent the means ± SD of three to four mice. *, $p < 0.01$.

after i.v. Ad administration is poorly understood. In the present study, although AdK7-L2 mediated higher luciferase expression and a higher accumulation of viral DNA in the liver than Ad-L2, it remains unclear why AdK7-L2 showed almost background levels of liver toxicity while Ad-L2 showed high toxicity. As reported previously, inflammatory cytokines, chemokines, and IFNs could be the mediators responsible for liver toxicity (2). IL-6 levels in the serum were the most strikingly different between AdK7-L2 and Ad-L2. Furthermore, IL-6 stimulated acute phase protein (serum amyloid A, fibrinogen, α_1-anti-trypsin, and α_1-acid glycoprotein) in rat and human hepatocytes (36, 37). Therefore, we next examined the effects of serum IL-6 on liver toxicity (Fig. 5). To do this, we used an anti-IL-6R Ab that inhibits the signal through the IL-6 receptor. The IL-6 receptor system consists of two functional molecules, an 80-kDa ligand-binding chain (IL-6R) and a 130-kDa nonligand-binding but signal-transducing chain (gp130). The anti-IL-6R Ab blocks the binding of IL-6 to the IL-6R (38, 39). The anti-IL-6R Ab or the control Ab was i.p. injected 1.5 h before the injection of Ad-L2. The AST levels in the serum and luciferase production in the liver were determined 48 h later. Administration of anti-IL-6R Ab significantly (~2-fold) reduced Ad vector-mediated AST levels in the serum compared with PBS or the control Ab (Fig. 5*A*). Importantly, anti-IL-6R Ab injection did not interfere with luciferase production in the liver (Fig. 5*B*). These results suggest that IL-6 signaling is involved in liver toxicity after i.v. administration of an Ad vector.

Discussion

In this study we found that the fiber-modified Ad vector containing the K7 peptide, which has high affinity with heparin sulfate, shows much lower serum IL-6 and liver toxicity than the conventional Ad vector. This improved characteristic is likely involved with the reduced biodistribution of the vector to the spleen compared with that of the conventional Ad vector. RT-PCR analysis showed that the spleen, not the liver, is the major site of cytokine, chemokine, and IFN (IL-6, IL-12, TNF-α, RANTES, MIP-2, IFN-α, IFN-β, and IFN-γ) production and that splenic conventional DC are the major effector cells of the innate immune response (at least IL-6 and IL-12 production) after i.v. administration of Ad vectors. We also showed that IL-6 signaling is involved in part with liver toxicity in response to Ad vectors. Importantly, this fiber-modified Ad vector containing the K7 peptide maintained higher transduction efficiency in all the organs examined, and the liver transduction was higher than that of the conventional Ad vector. Although there have been some reports that modified Ad vectors such as the pegylated Ad vector (18–21), the Ad vector containing the Ad type 35 fiber shaft and knob (40), and the triple mutant Ad vector with ablation of CAR, α_v integrin, and HSG binding (22) show decreased innate immune response and liver toxicity, these types of vector lose their transduction activity in vivo. To our knowledge, this is the first report of an Ad vector that maintains high transduction efficiency in vivo with reduced toxicity.

The fiber-modified Ad vector containing the K7 peptide has been developed to overcome the limitations imposed by the CAR dependence of Ad infection. Expanded and efficient gene transfer has been reported based on the use of mutant fiber proteins containing a stretch of lysine residues (23–25). However, there has been no report on the difference in gene transfer activity and toxicity in vivo between the conventional Ad vector and the fiber-modified Ad vector containing the K7 peptide. We have demonstrated that the fiber-modified Ad vector containing the K7 peptide mediates ~6-fold higher mouse liver transduction in response to i.v. administration than the conventional Ad vector (Fig. 1*A*). The amounts of fiber-modified Ad vector DNA in the liver after i.v. administration were also 5-fold higher than those with the conventional Ad vector (Fig. 1*B*). It has been reported that the interaction between the Ad type 5 fiber and the HSG of a hepatocyte is involved in the accumulation in the mouse liver and the cynomolgus monkey liver of systemically administered Ad vectors (41, 42). This fiber-modified Ad vector might mediate more efficient gene transduction through a much higher affinity for HSG. In contrast, the amounts of fiber-modified Ad vector DNA in the spleen after i.v. administration were 56-fold lower than those of the conventional Ad vector (Fig. 1*B*). Biodistribution of viral DNA reflects the total of receptor-mediated uptake and nonspecific uptake. Luciferase production in the cells mainly reflects receptor-mediated uptake. We previously reported that most Ad DNAs are taken up in the liver nonparenchymal cells, not parenchymal cells, after i.v. administration (22). In this study, the conventional Ad vector would also be taken up in the macrophages and DC by nonspecific uptake, resulting in significantly higher Ad DNA and lower luciferase production in the spleen. In contrast, the fiber-modified Ad vector would be taken up more in the liver via receptor-mediated uptake and nonspecific uptake, resulting in significantly lower Ad DNA in the other organs, especially the spleen. Even though the amount of AdK7-L2 uptake in the spleen, heart, lung, and kidney was less than that of Ad-L2 uptake, the amount of receptor-mediated uptake in these organs would be similar between Ad-L2 and AdK7-L2, suggesting that these vectors showed similar levels of luciferase production in the organs other than the liver.

The initiation of inflammatory innate immune responses occurs after the systemic administration of Ad vectors to animals and humans, and this toxicity limits the utility of Ad vectors for gene therapy. Increased cytokine/chemokine production after the injection of Ad vectors has been reported to be due to the introduction of input Ad vectors to Kupffer cells in the liver and DC (15, 17, 43–46). Detailed analysis of the organs responsible for the expression of cytokines, chemokines, and IFNs by RT-PCR suggests that their production can mainly be attributed to spleen cells (especially splenic conventional DC), not liver cells (Figs. 3 and 4), which is consistent with the recent report of Bart et al. (47). Therefore, interference with spleen distribution of the Ad vector should provide a useful method for safer gene therapy.

TLRs, which are crucial to the recognition of pathogen-associated molecular patterns, are expressed on various types of immune cells including macrophages, DC, B cells, splenic types of T cells, and even on nonimmune cells such as fibroblasts and epithelial cells (48). For example, HSV and CMV (dsDNA virus) activate inflammatory cytokines and type I IFN secretion by the stimulation of TLR9 (49–53). The innate immune receptor to the Ad has not yet been identified. It has not even been determined whether TLRs are involved in Ad-mediated innate immune response in vivo, although it has been reported that TLR signals are not involved in the DC maturation induced by the Ad vector (46). As shown in Fig. 3*B*, cytokine production against the Ad vector occurred mainly in conventional DC. It is noted that the TLR9-mediated innate immunity responses to DNA virus are cell type-specific and limited to plasmacytoid DC (50). The unidentified sensor receptor(s) for double-stranded Ad DNA or Ad capsid protein in conventional DC might play a critical role in the expression of inflammatory cytokines/chemokines and type I IFN. Although we have previously reported that large amounts of conventional Ad vector accumulate in nonparenchymal cells, including Kupffer cells and liver sinusoidal (endothelial) cells (22, 54), the expression of mRNA of cytokines, chemokines, and IFNs in the liver was weak after administration of the Ad vector (Fig. 3*B*). A lack of putative sensor receptor(s) against Ad or the inability of sensor receptor(s) to recognize Ad due to the specific cellular disposition of Ad in Kupffer cells might result in a reduced production of cytokines/chemokines/IFNs in the liver.

Another interesting finding is that the fiber-modified Ad vector containing the K7 peptide showed almost background levels of AST activity, which reflects liver toxicity (Fig. 2*B*). Histological analysis supported this finding (Fig. 2*C*). Because the K7-modified Ad vector showed higher transgene activity and a higher accumulation of viral DNA into the liver (Fig. 1), the transduction and distribution of the vector into the liver did not participate in liver toxicity. The cytokines/chemokines play a major causative role in liver damage associated with systemic Ad infusion as well as in the induction of an antiviral immune response (2). Ad-induced cytokines/chemokines recruit immune effector cells (neutrophils, monocyte/macrophages, and NK cells) to Ad-transduced cells (mainly liver), resulting in acute hepatic toxicity. Shayakhmetov et al. (35) have reported that hepatocytes and Kupffer cells trigger IL-1 transcription in liver tissue after i.v. administration of Ad vectors and that interference of IL-1-signaling reduces liver toxicity. We speculated that IL-6 could be the main mediator for hepatic toxicity because IL-6 is one of the main cytokines in the early stages of inflammation, IL-6 production by the fiber-modified Ad vector was much reduced (approximately a quarter) compared with that by the conventional Ad vector, and all of the cytokines/chemokines/IFNs we examined (including IL-6) were mainly produced by the spleen, not the liver. Treatment of the anti-IL-6R Ab decreased liver toxicity (Fig. 5), suggesting that IL-6 plays at least some role in liver toxicity induced by systemic injection of the Ad vector. Because the AST levels were only partially reduced by the treatment with the anti-IL-6R Ab, another mechanism such as IL-1 signaling, rapid Kupffer cell death (55, 56), activation of the liver endothelium (55), or other factors might be involved in the liver toxicity. Nevertheless, it is attractive that the K7-modified Ad vector did not show liver toxicity despite the higher transduction efficiency and higher accumulation of the vector into the liver (probably Kupffer cells).

Our present study provides new insight into the cellular biological mechanism related to the innate immune response and liver toxicity against the systemically administered Ad vector. Modification of vector tropism should contribute to safe gene therapy procedures.

Acknowledgments

We thank Misae Nishijima and Haiying Huang for their technical assistance.

Disclosures

The authors have no financial conflict of interest.

References

1. Muruve, D. A. 2004. The innate immune response to adenovirus vectors. *Hum. Gene Ther.* 15: 1157–1166.
2. Nazir, S. A., and J. P. Metcalf. 2005. Innate immune response to adenovirus. *J. Investig. Med.* 6: 292–304.
3. Yang, Y., H. C. Ertl, and J. M. Wilson. 1994. MHC class I-restricted cytotoxic T lymphocytes to viral antigens destroy hepatocytes in mice infected with E1-deleted recombinant adenoviruses. *Immunity* 1: 433–442.
4. Yang, Y., F. A. Nunes, K. Berencsi, E. E. Furth, E. Gonczol, and J. M. Wilson. 1994. Cellular immunity to viral antigens limits E1-deleted adenoviruses for gene therapy. *Proc. Natl. Acad. Sci. USA* 91: 4407–4411.
5. Yang, Y., Q. Su, and J. M. Wilson. 1996. Role of viral antigens in destructive cellular immune responses to adenovirus vector-transduced cells in mouse lungs. *J. Virol.* 70: 7209–7212.
6. Morral, N., R. J. Parks, H. Zhou, L. C. G. Schiedner, J. Quinones, F. L. Graham, S. Kochanek, and A. L. Beaudet. 1998. High doses of a helper-dependent adenoviral vector yield supraphysiological levels of α_1-antitrypsin with negligible toxicity. *Hum. Gene Ther.* 9: 2709–2716.
7. Morsy, M. A., M. Gu, S. Motzel, J. Zhao, J. Lin, Q. Su, H. Allen, L. Franlin, R. J. Parks, F. L. Graham, S. Kochanek, A. J. Bett, and C. T. Caskey. 1998. An adenoviral vector deleted for all viral coding sequences results in enhanced safety and extended expression of a leptin transgene. *Proc. Natl. Acad. Sci. USA* 95: 7866–7871.
8. Schiedner, G., N. Morral, R. J. Parks, Y. Wu, S. C. Koopmans, C. Langston, F. L. Graham, A. L. Beaudet, and S. Kochanek. 1998. Genomic DNA transfer with a high-capacity adenovirus vector results in improved in vivo gene expression and decreased toxicity. *Nat. Genet.* 18: 180–183.
9. Roberts, D. M., A. Nanda, M. J. Havenga, P. Abbink, D. M. Lynch, B. A. Ewald, J. Liu, A. R. Thorner, P. E. Swanson, D. A. Gorgone, et al. 2006. Hexon-chimaeric adenovirus serotype 5 vectors circumvent pre-existing anti-vector immunity. *Nature* 441: 239–243.
10. Farina, S. F., G. P. Gao, Z. Q. Xiang, J. J. Rux, R. M. Burnett, M. R. Alvira, J. Marsh, H. C. Ertl, and J. M. Wilson. 2001. Replication-defective vector based on a chimpanzee adenovirus. *J. Virol.* 75: 11603–11613.
11. Sakurai, F., H. Mizuguchi, and T. Hayakawa. 2003. Efficient gene transfer into human CD34$^+$ cells by an adenovirus type 35 vector. *Gene Ther.* 10: 1041–1048.
12. Vogels, R., D. Zuijdgeest, R. van Rijnsoever, E. Hartkoorn, I. Damen, M. P. de Bethune, S. Kostense, G. Penders, N. Helmus, W. Koudstaal, et al. 2003. Replication-deficient human adenovirus type 35 vectors for gene transfer and vaccination: efficient human cell infection and bypass of preexisting adenovirus immunity. *J. Virol.* 77: 8263–8271.
13. Holterman, L., R. Vogels, R. van der Vlugt, M. Sieuwerts, J. Grimbergen, J. Kaspers, E. Geelen, E. van der Helm, A. Lemckert, G. Gillissen, et al. 2004. Novel replication-incompetent vector derived from adenovirus type 11 (Ad11) for vaccination and gene therapy: low seroprevalence and non-cross-reactivity with Ad5. *J. Virol.* 78: 13207–13215.
14. Liu, Q., and D. A. Muruve. 2003. Molecular basis of the inflammatory response to adenovirus vectors. *Gene Ther.* 10: 935–940.
15. Zhang, Y., N. Chirmule, G. P. Gao, R. Qian, M. Croyle, B. Joshi, J. Tazelaar, and J. M. Wilson. 2001. Acute cytokine response to systemic adenoviral vectors in mice is mediated by dendritic cells and macrophages. *Mol. Ther.* 3: 697–707.
16. Clesham, G. J., P. J. Adam, D. Proudfoot, P. D. Flynn, S. Efstathiou, and P. L. Weissberg. 1998. High adenoviral loads stimulate NF-κB-dependent gene expression in human vascular smooth muscle cells. *Gene Ther.* 5: 174–180.
17. Lieber, A., C. Y. He, L. Meuse, D. Schowalter, I. Kirillova, B. Winther, and M. A. Kay. 1997. The role of Kupffer cell activation and viral gene expression in early liver toxicity after infusion of recombinant adenovirus vectors. *J. Virol.* 71: 8798–8807.

18. O'Riordan, C. R., A. Lachapelle, C. Delgado, V. Parkes, S. C. Wadsworth, A. E. Smith, and G. E. Francis. 1999. PEGylation of adenovirus with retention of infectivity and protection from neutralizing antibody in vitro and in vivo. *Hum. Gene Ther.* 10: 1349–1358.
19. Croyle, M. A., Q. C. Yu, and J. M. Wilson. 2000. Development of a rapid method for the PEGylation of adenoviruses with enhanced transduction and improved stability under harsh storage conditions. *Hum. Gene Ther.* 11: 1713–1722.
20. Croyle, M. A., H. T. Le, K. D. Linse, V. Cerullo, G. Toietta, A. Beaudet, and L. Pastore. 2005. PEGylated helper-dependent adenoviral vectors: highly efficient vectors with an enhanced safety profile. *Gene Ther.* 12: 579–587.
21. Mok, H., D. J. Palmer, P. Ng, and M. A. Barry. 2005. Evaluation of polyethylene glycol modification of first-generation and helper-dependent adenoviral vectors to reduce innate immune responses. *Mol. Ther.* 11: 66–79.
22. Koizumi, N., K. Kawabata, F. Sakurai, Y. Watanabe, T. Hayakawa, and H. Mizuguchi. 2006. Modified adenoviral vectors ablated for coxsackievirus-adenovirus receptor, α_v integrin, and heparan sulfate binding reduce in vivo tissue transduction and toxicity. *Hum. Gene Ther.* 17: 264–279.
23. Wickham, T. J., E. Tzeng, L. L. Shears II, P. W. Roelvink, Y. Li, G. M. Lee, D. E. Brough, A. Lizonova, and I. Kovesdi. 1997. Increased in vitro and in vivo gene transfer by adenovirus vectors containing chimeric fiber proteins. *J. Virol.* 11: 8221–8229.
24. Bouri, K., W. G. Feero, M. M. Myerburg, T. J. Wickham, I. Kovesdi, E. P. Hoffman, and P. R. Clemens. 1999. Polylysine modification of adenoviral fiber protein enhances muscle cell transduction. *Hum. Gene Ther.* 10: 1633–1640.
25. Koizumi, N., H. Mizuguchi, N. Utoguchi, Y. Watanabe, and T. Hayakawa. 2003. Generation of fiber-modified adenovirus vectors containing heterologous peptides in both the HI loop and C terminus of the fiber knob. *J. Gene Med.* 5: 267–276.
26. Mizuguchi, H., N. Koizumi, T. Hosono, N. Utoguchi, Y. Watanabe, M. A. Kay, and T. Hayakawa. 2001. A simplified system for constructing recombinant adenoviral vectors containing heterologous peptides in the HI loop of their fiber knob. *Gene Ther.* 8: 730–735.
27. Maizel, J. V., D. O. White, and M. D. Scharff. 1968. The polypeptides of adenovirus. I. Evidence for multiple protein components in the virion and a comparison of types 2, 7A, and 12. *Virology* 36: 115–125.
28. Xu, Z.-L., H. Mizuguchi, A. Ishii-Watabe, E. Uchida, T. Mayumi, and T. Hayakawa. 2001. Optimization of transcriptional regulatory elements for constructing plasmid vectors. *Gene* 272: 149–156.
29. Huard, J., H. Lochmuller, G. Acsadi, A. Jani, B. Massie, and G. Karpati. 1995. The route of administration is a major determinant of the transduction efficiency of rat tissues by adenoviral recombinants. *Gene Ther.* 2: 107–115.
30. Wood, M., P. Perrotte, E. Onishi, M. E. Harper, C. Dinney, L. Pagliaro, and D. R. Wilson. 1999. Biodistribution of an adenoviral vector carrying the luciferase reporter gene following intravesical or intravenous administration to a mouse. *Cancer Gene Ther.* 6: 367–372.
31. Worgall, S., G. Wolff, E. Falck-Pedersen, and R. G. Crystal. 1997. Innate immune mechanisms dominate elimination of adenoviral vectors following in vivo administration. *Hum. Gene Ther.* 8: 37–44.
32. Liu, Q., A. K. Zaiss, P. Colarusso, K. Patel, G. Haljan, T. J. Wickham, and D. A. Muruve. 2003. The role of capsid-endothelial interactions in the innate immune response to adenovirus vectors. *Hum. Gene Ther.* 14: 627–643.
33. Schiedner, G., S. Hertel, M. Johnston, V. Dries, R. N. Van, and S. Kochanek. 2003. Selective depletion or blockade of Kupffer cells leads to enhanced and prolonged hepatic transgene expression using high-capacity adenoviral vectors. *Mol. Ther.* 7: 35–43.
34. Engler, H., T. Machemer, J. Philopena, S. F. Wen, E. Quijano, M. Ramachandra, V. Tsai, and R. Ralston. 2004. Acute hepatotoxicity of oncolytic adenoviruses in mouse models is associated with expression of wild-type E1a and induction of TNF-α. *Virology* 328: 52–61.
35. Shayakhmetov, D. M., Z. Y. Li, S. Ni, and A. Lieber. 2005. Interference with the IL-1-signaling pathway improves the toxicity profile of systemically applied adenovirus vectors. *J. Immunol.* 174: 7310–7319.
36. Castell, J. V., T. Geiger, V. Gross, T. Andus, E. Walter, T. Hirano, T. Kishimoto, and P. C. Heinrich. 1988. Plasma clearance, organ distribution and target cells of interleukin-6/hepatocyte-stimulating factor in the rat. *Eur. J. Biochem.* 177: 357–361.
37. Geiger, T., T. Andus, J. Klapproth, T. Hirano, T. Kishimoto, and P. C. Heinrich. 1988. Induction of rat acute-phase proteins by interleukin 6 in vivo. *Eur. J. Immunol.* 18: 717–721.
38. Vink, A., P. Coulie, G. Warnier, J. C. Renauld, M. Stevens, D. Donckers, and J. Van Snick. 1990. Mouse plasmacytoma growth in vivo: enhancement by interleukin 6 (IL-6) and inhibition by antibodies directed against IL-6 or its receptor. *J. Exp. Med.* 172: 997–1000.
39. Boulanger, M. J., D. C. Chow, E. E. Brevnova, and K. C. Garcia. 2003. Hexameric structure and assembly of the interleukin-6/IL-6 α-receptor/gp130 complex. *Science* 300: 2101–2104.
40. Shayakhmetov, D. M., Z. Y. Li, S. Ni, and A. Lieber. 2004. Analysis of adenovirus sequestration in the liver, transduction of hepatic cells, and innate toxicity after injection of fiber-modified vectors. *J. Virol.* 78: 5368–5381.
41. Smith, T. A., N. Idamakanti, M. L. Rollence, J. Marshall-Neff, J. Kim, K. Mulgrew, G. R. Nemerow, M. Kaleko, and S. C. Stevenson. 2003. Adenovirus serotype 5 fiber shaft influences in vivo gene transfer in mice. *Hum. Gene Ther.* 14: 777–787.
42. Smith, T. A., N. Idamakanti, J. Marshall-Neff, M. L. Rollence, P. Wright, M. Kaloss, L. King, C. Mech, L. Dinges, W. O. Iverson, et al. 2003. Receptor interactions involved in adenoviral-mediated gene delivery after systemic administration in non-human primates. *Hum. Gene Ther.* 14: 1595–1604.
43. Schnell, M. A., Y. Zhang, J. Tazelaar, G. P. Gao, Q. C. Yu, R. Qian, S. J. Chen, A. N. Varnavski, C. LeClair, S. E. Raper, and J. M. Wilson. 2001. Activation of innate immunity in nonhuman primates following intraportal administration of adenoviral vectors. *Mol. Ther.* 3: 708–722.
44. Morral, N., W. K. O'Neal, K. M. Rice, P. A. Piedra, E. Aguilar-Cordova, K. D. Carey, A. L. Beaudet, and C. Langston. 2002. Lethal toxicity, severe endothelial injury, and a threshold effect with high doses of an adenoviral vector in baboons. *Hum. Gene Ther.* 13: 143–154.
45. Reid, T., E. Galanis, J. Abbruzzese, D. Sze, L. M. Wein, J. Andrews, B. Randlev, C. Heise, M. Uprichard, M. Hatfield, et al. 2002. Hepatic arterial infusion of a replication-selective oncolytic adenovirus (dl1520): phase II viral, immunologic, and clinical endpoints. *Cancer Res.* 62: 6070–6079.
46. Philpott, N. J., M. Nociari, K. B. Elkon, and E. Falck-Pedersen. 2004. Adenovirus-induced maturation of dendritic cells through a PI3 kinase-mediated TNF-α induction pathway. *Proc. Natl. Acad. Sci. USA* 1001: 6200–6205.
47. Bart, D. G., S. Jan, V. L. Sophie, L. Joke, and C. Desire. 2005. Elimination of innate immune responses and liver inflammation by PEGylation of adenoviral vectors and methylprednisolone. *Hum. Gene Ther.* 16: 1439–1451.
48. Akira, S., S. Uematsu, and O. Takeuchi. 2006. Pathogen recognition and innate immunity. *Cell* 124: 783–801.
49. Lund, J., A. Sato, S. Akira, R. Medzhitov, and A. Iwasaki. 2003. Toll-like receptor 9-mediated recognition of herpes simplex virus-2 by plasmacytoid dendritic cells. *J. Exp. Med.* 198: 513–520.
50. Hochrein, H., B. Schlatter, M. O'Keeffe, C. Wagner, F. Schmitz, M. Schiemann, S. Bauer, M. Suter, and H. Wagner. 2004. Herpes simplex virus type-1 induces IFN-α production via Toll-like receptor 9-dependent and -independent pathways. *Proc. Natl. Acad. Sci. USA* 101: 11416–11421.
51. Krug, A., A. R. French, W. Barchet, J. A. Fischer, A. Dzionek, J. T. Pingel, M. M. Orihuela, S. Akira, W. M. Yokoyama, and M. Colonna. 2004. TLR9-dependent recognition of MCMV by IPC and DC generates coordinated cytokine responses that activate antiviral NK cell function. *Immunity* 21: 107–119.
52. Krug, A., G. D. Luker, W. Barchet, D. A. Leib, S. Akira, and M. Colonna. 2004. Herpes simplex virus type 1 activates murine natural interferon-producing cells through toll-like receptor 9. *Blood* 103: 1433–1437.
53. Tabeta, K., P. Georgel, E. Janssen, X. Du, K. Hoebe, K. Crozat, S. Mudd, L. Shamel, S. Sovath, J. Goode, et al. 2004. Toll-like receptors 9 and 3 as essential components of innate immune defense against mouse cytomegalovirus infection. *Proc. Natl. Acad. Sci. USA* 101: 3516–3521.
54. Koizumi, N., H. Mizuguchi, F. Sakurai, T. Yamaguchi, Y. Watanabe, and T. Hayakawa. 2003. Reduction of natural adenovirus tropism to mouse liver by fiber-shaft exchange in combination with both CAR- and α_v integrin-binding ablation. *J. Virol.* 24: 13062–13072.
55. Schiedner, G., W. Bloch, S. Hertel, M. Johnston, A. Molojavyi, V. Dries, G. Varga, N. Van Rooijen, and S. Kochanek. 2003. A hemodynamic response to intravenous adenovirus vector particles is caused by systemic Kupffer cell-mediated activation of endothelial cells. *Hum. Gene Ther.* 14: 1631–1641.
56. Manickan, E., J. S. Smith, J. Tian, T. L. Eggerman, J. N. Lozier, J. Muller, and A. P. Byrnes. 2006. Rapid Kupffer cell death after intravenous injection of adenovirus vectors. *Mol. Ther.* 13: 108–117.

Journal of Organ Dysfunction, 2007; 3: 164–182

informa
healthcare

REVIEW ARTICLE

Study of hepatocytes using RNA interference

SHINGO NIIMI[1], MIZUHO HARASHIMA[2], MASASHI HYUGA[1] and TERUHIDE YAMAGUCHI[1]

[1]*Division of Biological Chemistry and Biologicals, National Institute of Heath Sciences, Tokyo, Japan, and* [2]*Department of Nutrition and Physiology, Nihon University College of Bioresource Sciences, Fujisawa, Japan*

Abstract

RNA interference (RNAi) is the process of sequence-specific gene silencing, initiated by small double-stranded RNA homologous in sequence to the target gene. Various factors involved in the regulation of hepatocyte function have been identified using RNAi, indicating that RNAi is a useful strategy for characterization. There has been some success in treating experimental liver dysfunction using RNAi in several model systems, suggesting a promising new therapeutic strategy. A number of groups have also demonstrated that RNAi can interfere with hepatitis C virus and hepatitis B virus gene expression and replication in several model systems, suggesting a new approach for the treatment of these viral diseases. This review summarizes studies of hepatocytes using RNAi.

Key words: *Hepatitis B virus, hepatitis C virus, hepatocyte, RNA interference, short hairpin RNA, small interfering RNA*

Introduction

RNA interference (RNAi) is a process by which double-stranded RNA (dsRNA) triggers sequence-specific silencing of homologous genes (1). This process is evolutionarily conserved through a variety of eukaryotic organisms (2,3). The process is initiated by the RNase III-like nuclease Dicer, which promotes progressive cleavage of long dsRNAs into 21–27-nucleotide (nt) short interfering RNA (siRNA) with two-nt 3′-overhangs. Subsequently, the siRNA unwinds and binds to an activated RNAi-induced silencing complex. Single-stranded (ss) siRNAs then bind to target sequences based on sequence complementarity, resulting in cleavage of the target sequence (4–10). Although first discovered in the worm Caenorhabditis elegans, it was demonstrated soon after that RNAi can be induced in various mammalian cells by introducing synthetic 21-nt siRNA to obtain strong and specific suppression (knockdown) of gene expression (11). Exposure to dsRNAs >30 bp in length induces an antiviral interferon response that generally represses mRNA translation through the activation of dsRNA-dependent protein kinase (PKR) and 2′,5′-oligoadenylate synthetase (2′,5′-OAS) (12,13). This kind of RNAi is highly sequence-specific, with even a single mismatch between the siRNA and its target sequence being able to dramatically decrease the efficacy of RNA degradation. Systems for stable and continuous expression of short hairpin RNA (shRNA) and duplex siRNA transcribed in vitro and in vivo from DNA templates also suppress gene expression in mammalian cells (14–17). From a practical perspective, RNAi has become a powerful non-destructive, non-mutating tool for the analysis of gene function in different living systems (18–20) and one that holds great promise for the treatment of many infectious diseases and cancers (21–24).

In this review, efforts to identify factors involved in the regulation of hepatocyte function, and to treat experimental liver failure, hepatitis C virus (HCV), and hepatitis B virus (HBV) disease using RNAi are summarized.

Correspondence: Shingo Niimi, PhD, Division of Biological Chemistry and Biologicals, National Institute of Health Sciences, 1-18-1 Kamiyoga, Setagaya-ku, Tokyo 158-8501, Japan. Fax: +81 3 3700 9347. E-mail: niimi@nihs.go.jp

ISSN Print 1747-1060 ISSN Online 1747-1079
DOI: 10.1080/17471060701286559

Identification of factors involved in the regulation of hepatocyte function using RNAi

Various factors involved in the regulation of hepatocyte function using RNAi are described below and summarized in Table I.

Annexin A3

Small hepatocytes are a minor subpopulation of cells with high replication potential in defined media (25–27). After 1 day of culture, small hepatocytes express universal hepatocyte markers, differentiating into cells expressing differentiated hepatocyte marker or biliary cell marker protein (28). The molecular mechanism regulating these characteristic phenotypes is yet to be elucidated. Niimi et al. (29) attempted to identify proteins specifically expressed in isolated small, but not parenchymal, isolated rat hepatocytes using a proteomic approach. Annexin A3 was only expressed in the small rat hepatocytes. Annexin A3 siRNA inhibited stimulation of DNA synthesis by hepatocyte growth factor (HGF) and epidermal growth factor (EGF), suggesting that annexin A3 is necessary for DNA synthesis in cultured parenchymal rat hepatocytes (30).

Coactivator-associated arginine methyltransferase

De novo glucose production, e.g. gluconeogenesis, represents a key feature of hepatic metabolism under fasting conditions to maintain blood glucose levels and energy substrates for brain function (31). Phosphoenolpyruvate carboxikinase (PEPCK) and glucose-6-phosphatase (G6Pase) genes have been identified as the rate-limiting steps in the gluconeogenic pathways. Transcription of these genes is stimulated by glucagon via intracellular cyclic adenosine monophosphate/protein kinase A (PKA) (31–33). Coactivator-associated arginine methyltransaferase (CARM1) was originally identified as a co-factor for the estrogen receptor, working in combination with members of the p160 family of nuclear receptor co-factors (e.g. steroid receptor coactivator-1/TIF2/glucocorticoid receptor interaction protein 1), as well as the cAMP-responsive element binding factor-binding protein CBP/P300 (34,35).

CARM1 siRNA inhibited PKA-induced PEPCK and G6Pase promoter activities in HepG2 cells, suggesting that CARM1 plays a role in the stimulation of PEPCK and G6Pase gene expression by PKA (36).

Aryl hydrocarbon receptor

It has been suggest in numerous reports (37–44) that 2,3,7,8-tetrachlorodibenzo-*p*-dioxin (TCCD) promotes Fas-mediated apoptosis. The aryl hydrocarbon receptor (AhR) is a cytosolic, ligand-activated transcription factor that regulates the expression of several genes in response to polycyclic and halogenated aromatic hydrocarbon ligands, such as TCCD (45,46).

Table I. Regulation of hepatocyte function using RNAi.

Target gene	Regulation of hepatocyte function	Reference
Annexin A3	Inhibition of Stimulation of DNA synthesis by HGF and EGF	30
CARM1	Inhibition of PKA-induced PEPCK and G6Pase promoter activities	36
AhR	Protection of Jo2-induced lethality	47
MIZ-1	Inhibition of T113242-dependent activation of LDL gene and cell growth	49
LRH-1	Down-regulation of APOA1 gene expression	51
GATA-4	Inhibition of Epo gene expression	59
FOXO1	Decrease of reporter activity derived from CAR	80
ARH	Reduction of LDL internalization	85
Pim-3	Attenuation of proliferation rates, stimulation of cell death	90
GR, MR	Abolition of UDCA protection against TGF-β1-mediated apoptosis, decrease of protective effect of UDCA in TGF-β1-associated caspase activation and TGF-β1-induced E2F-l/Mdm/p53 apoptotic pathway	110
cFLIP	Reversion of anti-apoptotic effect of Dex against TNF-α+Actinomycin D-induced apoptosis	117
MLCK	Inhibition of DNA replication, expression of cdk1 and phosphorylation of p70S6K induced by EGF	121
ERK2	Inhibition of phosphorylation of p70S6K induced by EGF	121
p70S6K	Suppression of stimulation of DNA synthesis by EGF	121
EndoG	Suppression of decrease in TUNEL-positive nuclei	132
DNMT3B	Upregulation or downregulation of some important developmental genes and tumor-related genes	135
PTEN	Prevention of TNF-activated cell death signaling pathways, prevention of promotion of Bax-induced mitochodrial injury by TNF, prevention of induction of cell death by ethanol	147
TLR3, TRIF	Inhibition of induction of IFN-β promoter activity and ISG56mRNA transcription in response to Poly (I-C)	158
RIG-1	Inhibition of induction of IFN-β, NF-κB-dependent PRDII promoters, inhibition of transcription of ISG mRNA in response to Sen V	158
TLR3	Override of induction of IFN-β and cell cycle delay	175

Park et al. (47) investigated the role of AhR in Fas-mediated apoptosis by using adenovirus (Ad) expressing siRNA against AhR. Treatment of mice with siRNA protects against Jo2-induced lethality. Furthermore, AhR expression in primary hepatocytes from $AhR^{-/-}$ mice increases Fas ligand-induced apoptosis. These findings indicate that AhR predisposes hepatocytes to Fas-mediated apoptosis and subsequent lethality in animals.

Myc-interacting protein 1

Myc-interacting protein 1 (MIZ-1) was identified by virtue of its ability to bind to Myc.

MIZ-1 is sequestered in the cytoplasm by association with microtubules. Upon drug-induced microtubule depolymerization, MIZ is free to enter the nucleus where it binds to target sequences, such as low-density lipoprotein receptor (LDLR) gene promoter, and activates transcription (48).

Using the microtubule disrupting agent T113242, Ziegelbauer et al. (49) demonstrated that MIZ-1 siRNA inhibited T113242-dependent activation of the LDL gene in HepG2 cells, inhibiting cell growth.

Liver receptor homolog-1

The orphan nuclear receptor liver receptor homolog-1 (LRH-1) regulates the scavenger receptor class B type 1 gene (50) that mediates selective uptake of high-density lipoprotein (HDL) and plays a key role in reverse cholesterol uptake. Apolipoprotein A1 (APOA1), the major protein component of HDL, plays a role in reverse cholesterol transport.

Delerive et al. (51) demonstrated that LRH-1 siRNA downregulated APOA1 gene expression in HepG2 cells, suggesting that LRH-1 plays a role in the stimulation of APOA1 gene expression.

GATA-4

Erythropoietin (Epo) production sites developmentally change and switch from the fetal liver to adult kidney (52,53). GATA transcriptional factors belong to the family of zinc DNA-binding proteins and play critical roles in cell growth and differentiation (54,55). GATA-4, one of six members of the GATA family, is expressed in the liver during murine embryogenesis (56). Expression of GATA-4 is detectable late in gestation only in endothelial/epithelial cells surrounding the hepatic vessels. In a recent study (57) it was demonstrated that GATA-4 cooperates with hepatocyte nuclear factor-3 to stimulate the albumin gene in liver progenitor cells. Hep3B is a hepatoma cell line similar to fetal hepatocytes and is generally accepted as a good model for hepatic Epo gene regulation (58)

Dame et al. (59) demonstrated that GATA-4 shRNA inhibited Epo gene expression, suggesting that GATA-4 plays a critical role in Epo gene regulation in Hep3B cells.

FOXO1

FOXO1, a forkhead transcription factor, activates gluconeogenic genes by binding to an insulin response element (IRS) located on those genes (60–64). Insulin phosphorylates FOXO1 via a phosphatidylinositol 3-kinase–Akt pathway (60,65, 66) and inactivates FOXO1 by decreasing the binding affinity of FOXO1 to IRS and/or exporting FOXO1 from the nucleus (67–70). Insulin represses the induction of drug-metabolizing enzymes by certain drugs in diabetic livers (71–73) and rat primary hepatocytes (74–76). In contrast, the nuclear receptor CAR plays a central role in the induction of drug-metabolizing enzymes, such as cytochrome P450s, by certain drugs (77–79).

Kodama et al. (80) demonstrated that FOXO1 siRNA decreased reporter activity derived from CAR in HepG2 cells, suggesting that FOXO1 may play a role in regulating CAR-mediated transactivation in HepG2 cells.

Autosomal recessive hypercholesterolemia

LDLR plays a pivotal role in the regulation of cholesterol metabolism (81). LDLR is a ubiquitous cell surface glycoprotein which is able to bind LDL, the major cholesterol transport vesicle in plasma. The autosomal recessive hypercholesterolemia (ARH) protein contains an $\approx$130-residue phosphotyrosine-binding domain evolutionarily related to other adaptor proteins. These adaptor proteins, including ARH, bind the conserved sequence motif NPXY located in the cytoplasmic domain of various cell surface receptors and mediate several functions, including trafficking and endocytosis. The LDLR cytoplasmic tail contains a single NPXY motif required for clustering and endocytosis of the receptor in fibroblasts. Transformed lymphocytes and monocyte-derived macrophage obtained from ARH patients are unable to take up and degrade ^{125}I-LDL (82–84), suggesting that ARH is required for efficient endocytosis of LDL in these cells.

A quantitative immunofluorescence analysis performed by Sirinian et al. (85) indicated that ARH siRNA causes a reduction in LDL internalization, suggesting that ARH is an endocyte-sorting adaptor that actively participates in internalization of the LDL–LDLR complex.

Pim-3

Among human cancers, the greatest number of deaths result from hepatocellular carcinoma (HCC). Most cases of HCC arise from chronic infection with human HBV or HCV (86). Host responses are assumed to be involved in the development of HCC, as these viruses lack apparent oncogenes and infected patients develop HCC after suffering from chronic hepatitis-related pathology (87,88).

Nakamoto et al. (89) used a mouse model of HCC, established using an HBV surface antigen (HBsAg) transgenic mouse, to compare gene expression in the non-tumor portion of this disease, examining pre-malignant lesions and normal tissue (90). Gene expression of Pim-3, which is involved in EWS/ETS-mediated malignant transformation of NIH 3T3 cells (91), was enhanced in pre-malignant regions. siRNA against Pim-3 attenuated proliferation rates and caused cell death in HuH7 cells, suggesting that Pim-3 can cause autonomous cell proliferation or prevent apoptosis in HuH7 cells.

Glucocorticoid receptor and mineralocorticoid receptor

E2F-1 is the best-characterized member of the E2F family of transcriptional factors, regulating a number of genes involved in apoptosis (92,93). Unbound E2F-1 modulates transforming growth factor (TGF)-β1-induced apoptosis in hepatic cells (94–96). The ability of E2F-1 to promote apoptosis involves stabilization of tumor suppressor protein p53 via transcription of $p14^{ARF}$, which markedly inhibits the p53 repressor Mdm-2 (93,94). Ursodeoxycholic acid (UDCA) interrupts the apoptotic pathway by interfering with mitochondrial pathways in both hepatic and non-hepatic cells (97–100), and interfering with the E2F-1/p53 apoptotic pathway (94). UDCA also modulates activation of glucocorticoid receptor (GR) (101), probably by interaction with distinct regions of its ligand-binding domain, thus suppressing, for example, nuclear factor (NF)-κB-dependent transcription (102). Dexamethasone (Dex), a strong activator of GR, prolongs cell viability, inhibits the development of apoptotic morphology, and stabilizes the expression of procaspase-3 in both human and rat hepatocytes (103), plus inhibiting TGF-β1-induced apoptosis in rat hepatoma cells (104). Mineralocorticoid receptor (MR) also has a predominantly anti-apoptotic role in several neuronal systems (105–109).

Sola et al. (110) demonstrated that both GR and MR siRNAs abolished UDCA protection against TGF-β1-mediated apoptosis. Both GR and MR siRNAs also decreased the protective effect of UDCA in TGF-β1-associated caspase activation and the TGF-β1-induced E2F-1/Mdm/p53 apoptotic pathway. These results demonstrate that UDCA protects against apoptosis through GR and MR, and that the E2F-1/Mdm/p53 apoptotic pathway appears to be a prime target for UDCA-induced GR and MR activation.

FLICE inhibitory protein

Hepatocyte apoptosis can be initiated by exposure to toxic substances or ligation of members of the death receptor family, including tumor necrosis factor (TNF)-α receptor (TNF-R) and Fas (111). Dex inhibits apoptosis in primary human and rat hepatocytes (103). Although several sets of genes have been characterized as being involved in the anti-apoptotic effect of Dex in spontaneous apoptosis of cultured primary hepatocytes (112), the mechanism behind the anti-apoptotic effect of Dex has rarely been investigated in death receptor-mediated apoptosis. FLICE inhibitory protein (cFLIP) is a cellular inhibitor for caspase-8 activation in death receptor-induced apoptosis (113), inhibiting apoptosis induced by death receptor-activating ligands, such as TNF-α, FasL (114), and TNF-related apoptosis-inducing ligand (114–116).

Oh et al. (117) found that Dex upregulated cellular cFLIP expression. siRNA against cFLIP reversed the anti-apoptotic effect of Dex by increasing caspase-8 activation in TNF-α + actinomycin D-induced hepatocyte apoptosis. These results indicate that Dex exerts a protective role in death receptor-induced hepatocyte apoptosis by upregulating cFLIP expression.

Myosin light-chain kinase, extracellular signal-regulated kinase-2 and p70S6K

Inhibition of myosin light-chain kinase (MLCK) blocks DNA synthesis in hepatocytes cultured on high-density fibronectin (118). p70S6K has been implicated in the regulation of hepatocyte proliferation, and extracellular signal-regulated kinase (ERK) has been reported to phosphorylate p70S6K in hepatocytes (119,120).

Bessard et al. (121) investigated the role of MLCK in cell-cycle progression in cultured rat hepatocytes by using siRNAs against MLCK, ERK2, and p70S6K. MLCK siRNA inhibited DNA replication and the expression of cdk1, a marker of S phase progression, and cyclin E, a major player in initial S progression in EGF-treated cells. ML7, an inhibitor of MLCK, inhibited cyclin D1, an important regulator of late G1 phase progression at the mRNA level. Both MLCK and ERK2 siRNAs inhibited

phosphorylation of p70S6K induced by EGF. p70S6K siRNA suppressed stimulation of DNA synthesis by EGF. These results underline the fact that there is an MLCK-dependent restriction point in G1/S transition which occurs downstream of ERK2 by means of regulation of p70S6K activation.

Endonuclease G

Apoptosis is a major cellular response against oxidative stress, the mechanisms of which have been extensively discussed (122–127). Inhibition of catalase and glutathione peroxidase activities by 3-amino-1,2,4-triazole (ATZ) and mercaptosuccinic acid (MS) caused sustained endogenous oxidative stress and apoptotic cell death without caspase-3 activation, respectively in rat primary hepatocytes (128,129). Endonuclease G (EndoG), an executive cause of DNA fragmentation, has been shown to be caspase-independently translocated from mitochondria to nuclei in response to apoptotic stimuli, with subsequent induction of nucleosomal DNA fragmentation (130,131).

Ishihara et al. (132) demonstrated that EndoG siRNA significantly suppressed decreases in terminal deoxynucleotide transferase-mediated dUTP nick-end labeling (TUNEL)-positive nuclei, indicating that EndoG is involved in DNA fragmentation induced by ATZ and MS.

De novo methyltransferase 3B

De novo methyltransferase 3B (DNMT3B) is one of several DNMT3 isoforms involved in establishing genomic methylation patterns (133,134). Expression of DNMT3B was minimally observed in some non-tumor livers and normal liver cell lines, but was much higher in HCCs and in HCC cell lines, suggesting that DNMT3B has a role relevant to liver cancer.

Jun et al. (135) investigated the influence of DNMT3B in gene expression by using siRNA against DNMT3B in the human HCC cell line SMMC-7721. Microarray analysis identified 26 down- and 115 upregulated genes in cells treated with DNMT3B siRNA. These genes included important developmental and tumor-related genes, such as SNCG, NOTCH1, MBD3, WNT11, MAOA, and FACL4.

Phosphate and tensin homolog deleted from chromosome 10

TNF is a central agent in the genesis of alcoholic liver disease (136–140). When hepatocytes are exposed to ethanol, they exhibit increased sensitivity to TNF-induced cell death (141,142). Activated Akt acts as an inhibitor of apoptosis (143–145) and phosphatidylinositol 3,4,5-triphosphate (PIP_3) is necessary for its activation. TNF receptor (TNFR) stimulates Akt activation by activating phosphatidylinositol 3-kinase, phosphorylating PIP_2 to generate PIP_3. When primary hepatocytes and the hepatoma cell line HepG2E47 are exposed to ethanol, these cells exhibit a decrease in stimulation of Akt activity by TNF (146). In contrast, phosphate and tensin homolog deleted from chromosome 10 (PTEN) is a tyrosine phosphatase with dual protein and lipid phosphatase activity. PTEN recognizes PIP_3 as a substrate and removes the D3 phosphate from the inositol ring, which is likely to cause a decrease in the concentration of PIP_3 and thus inhibit TNF-stimulated Akt activity.

Shulga et al. (147) investigated the role of PTEN in ethanol-induced signaling pathways that elicit sensitization to TNF cytotoxicity using siRNA against PTEN. PTEN expression increased in ethanol-exposed HepG2E47 cells. PTEN siRNA prevented TNF-activated cell death signaling pathways, such as p38 activation, apoptosis signaling kinase 1 phosphorylation, and translocation of Bax from cytosol to the mitochondria in ethanol-exposed cells. PTEN siRNA also prevents TNF from promoting Bax-induced mitochondrial injury, such as the loss of cytochrome C from mitochondria and localization to the cytosol, plus cell death, in ethanol-exposed cells. These findings indicate that PTEN is involved in the increased sensitivity of ethanol-exposed cells to TNF-induced cytotoxicity.

Toll-like receptor-3, Toll-interleukin-1 receptor domain-containing adaptor-inducing interferon-β and retinoic acid-inducible gene 1

Innate cellular antiviral defenses are likely to influence the outcome of infections by many human viruses. Toll-like receptors (TLRs) are a class of pathogen-associated molecular partners that detect infection by many types of pathogen, including viruses (148). TLR3 is engaged specifically by dsRNA present either in the viral genome or generated during viral replication, and is involved in cellular recognition of RNA viruses and the induction of type 1 interferon (IFN) responses (149). TLR-3 signaling requires the adaptor protein Toll-interleukin (IL)-1 receptor (TIR) domain-containing adaptor-inducing IFN-β (TRIF)/TIR domain-containing adaptor molecule 1 (TICAM1) (150–153). However, it has been indicated in several recent studies (154–156) that viral infection can also activate the host response through TLR3-independent pathways. Retinoic acid-inducible gene

1 (RIG-1) is a cytoplasmic RNA helicase that putatively binds viral dsDNA within its helicase domain, resulting in activation of IFN regulatory factor 3 and NF-κB (157). Although the liver is a very important site of persistent viral infection in humans, very little is known about how these pathways function, specifically in hepatocytes.

Li et al. (158) investigated antiviral signaling pathways active in the hepatocyte-derived cell line PH5CH8 using siRNAs against TLR3, TRIF, and RIG-1. PH5CH8 cells are derived from non-neoplastic hepatocytes transformed with T antigen from non-neoplastic liver tissue of a HCV-related HCC patient (159,160). Poly (I-C) activated the IFN-β promoter, resulting in robust expression of IFN-stimulated genes (ISG) in the cells. TLR3 siRNA or TRIF siRNA inhibited induction of IFN-β promoter activity and ISG56 mRNA transcription in response to Poly (I-C), but not Sendai virus (Sen V). RIG-1 siRNA inhibited induction of IFN-β, NF-κB-dependent PRDII promoters, and transcription of ISG mRNA in response to Sen V. However, RIG-1 siRNA did not inhibit Poly (I-C) induction of ISG56 transcription. These findings indicate that hepatocytes contain two distinct antiviral signaling pathways leading to expression of type 1 IFNs, one dependent on TLR3 and the other on RIG-1, with little evidence of significant cross-talk between them.

NS5B

Although persistent infection with HCV is a major cause of various human liver diseases, as described below, the molecular mechanisms remain elusive. Unregulated cell-cycle progression may be a cause of malignant transformation of normal cells. Inhibition of cell-cycle progression through the S phase may cause replication errors during DNA replication, inducing genomic instability and malignant transformation. Therefore, it is important to clarify the effect of HCV proteins on cell-cycle progression in order to determine molecular mechanisms underlying the pathogenesis of HCV. Although it was suggested in a number of previous reports (161–164) that several HCV proteins are involved in modulating cell-cycle progression, the conclusions of those studies are still being debated (165–171). However, several findings (159, 172–174) indicate that the PH5CH8 cell line described above is more relevant for studying the role of HCV proteins during hepatocarcinogenesis.

Naka et al. (175) investigated the effect of HCV NS5B, an RNA-dependent RNA polymerase, on the pathogenesis of HCV using siRNA against TLR3 in the PH5CH8 cell line. Infection with a retroviral vector encoding HCV NS5B delayed cell-cycle progression through the S phase and promoted IFN-β production in the PH5CH8 cell line, and an anti-IFN-β antibody restored the cell-cycle delay. TLR3 siRNA overrode the induction of IFN-β and the cell-cycle delay. These findings indicate that NS5B delays cell-cycle progression by inducing IFN-β through activation of the TLR signaling pathway.

Treatment of experimental liver dysfunction by RNAi

RNAi targeting the key factors involved in the development of liver dysfunction can effectively treat experimentally induced dysfunction in several model systems. Several of these findings are described below and summarized in Table II. RNAi represents a promising new strategy for the treatment of liver dysfunction.

Rejection after hepatocyte transplantation/Fas

Fas-mediated apoptosis has also been implicated in hepatocyte apoptosis upon allogenic hepatocyte transplantation (176). Blockade of Fas and Fas ligand interactions promotes repopulation of allogenic liver cells in recipient spleen (177).

Wang et al. (178) investigated the protective effects of siRNA against Fas on allogenic hepatocytes transplanted into mouse spleen. Transplantation of

Table II. Treatment of experimental liver dysfunction using RNAi.

Target gene	Treatment of liver dysfunction	Model	Reference
Fas	Decrease of apoptosis, improvement of decrease of survival	Rejection after hepatocyte transplantation	178
Caspase 8	Prevention of apoptosis, reduction of liver damage, improvement of decrease of survival	Fas-mediated ALF	184
TGF-βII	Suppression of expression of several TGF-β-responsive genes, prevention of cell damage, prevention of release of aminotransferases, improvement of decrease of survival	Fas-mediated acute liver injury and ALF	188
Fas	Abrogation of necrosis and inflammatory infiltration, prevention of elevation of serum transaminases, improvement of decrease in survival	Fas-mediated liver failure and fibrosis	194

hepatocytes treated with Fas siRNA into recipient spleen after 21 days resulted in a decrease in apoptosis of ≈50% and increased survival of transplanted hepatocytes approximately twofold. These results suggest that Fas silencing by RNAi holds promise for inhibiting acute rejection after hepatocyte transplantation.

Fas-mediated acute liver failure/caspase-8

Acute liver failure (ALF) is a dramatic clinical syndrome in which a previously normal liver fails within days or weeks and is associated with high mortality rates. In ALF, signals from death receptors, such as Fas (CD95), TNF-α, and TNF-related apoptosis-inducing ligand, trigger suicide pathways (179–181), leading to the activation of caspase cascades that subsequently induce the apoptotic death of hepatocytes. Consequently, an attractive strategy to treat patients with ALF would be to inhibit death receptor-mediated apoptosis to maintain liver function and save the organ.

Zender et al. examined the efficacy of siRNA against caspase 8, a key enzyme in death receptor-mediated apoptosis (182,183), to protect against ALF using different mouse models (184). Systematic application of caspase 8 siRNA prevents Fas (CD95)-mediated apoptosis of hepatocytes. Protection of hepatocytes by caspase 8 siRNA results in reduced liver damage after application of activating anti-Fas (CD95) antibody (Jo2) or Ad-expressing Fas ligand (AdFasL). Survival improved after delayed treatment of mice with caspase 8 siRNA following administration of AdFasL or Ad wild type. These findings demonstrate the therapeutic potential of RNAi targeting caspase 8 in ALF.

Fas-mediated ALF and ALF/ TGF-β receptor II

In the liver, TGF-β plays an essential role in hepatocyte apoptosis, growth inhibition, and the progression of fibrogenesis. The pathology underlying ALF involves overefficient apoptosis and the inhibition of hepatocyte regeneration associated with TGF-β signaling (185,186). TGF-β receptor II (TGF-βR-II) is considered a key target for interfering with TGF-β signaling (187). However, the potential use of in vivo RNAi in therapy and analytical activity by suppressing TGF-βR-II in the TGF-β signaling pathway has not yet been established or documented.

To approach this problem, Mizuguchi et al. (188) investigated the effect of the shRNA against TGF-βR-II using hepatocyte injury in mouse BNL, CL.2 cells, and liver injury models. TGF-βR-II shRNA suppressed the activation of SMAD2 and the induction of several TGF-β-responsive genes by TGF-β1 in the mouse cells. TGF-βR-II shRNA suppressed inhibition of cell proliferation and stimulation of apoptosis by TGF-β1. In a mouse acute liver injury model induced by Jo2 antibody, TGF-β-RII shRNA suppressed several TGF-β-responsive genes, prevented cell damage, and prevented the release of aminotransferases from damaged hepatocytes. In a survival study with Fas-mediated ALF, TGF-β-RII shRNA protected mice from death. These findings indicate that the use of shRNA targeting TGF-βR-II has great potential as an analytic tool for TGF-βR-II in TGF-β signaling and gene-specific therapeutics for human disorders.

Fas-mediated liver failure and fibrosis/Fas

Fas-mediated hepatocyte apoptosis is implicated in a broad spectrum of liver diseases, including the development of liver fibrosis in chronic hepatitis (189–192). Fas-deficient lpr mice survive challenge with factors that induce fulminant hepatitis in normal mice (190,193), and show reduced fibrosis after chronic hepatic insult (191).

Song et al. (194) investigated the effect of siRNA against Fas for protecting mice from liver failure and fibrosis in two models of autoimmune hepatitis. Hepatocytes isolated from mice treated with Fas siRNA were resistant to apoptosis when exposed to Jo2 in vitro or co-cultured with hepatic mononuclear cells harvested from concanavalin A (ConA)-treated mice. Hepatocytes from mice treated with Fas siRNA were resistant to cytolysis by hepatic mononuclear cells from ConA-treated mice. Treatment with Fas siRNA 1 day before ConA treatment abrogated hepatocyte necrosis and inflammatory infiltration, as well as almost completely preventing elevation of serum transaminases. Treatment with Fas siRNA, beginning 1 week after the initiation of weekly ConA treatment, protected mice from liver fibrosis. In a more aggressive hepatitis model using a Fas-specific antibody, 82% of mice treated with Fas siRNA survived for 10 days, whereas all control mice died within 3 days. These results indicate that siRNA-directed Fas silencing may be of therapeutic value in preventing liver injury by protecting hepatocytes from cytotoxicity.

Inhibition of HCV gene expression and replication by RNAi

HCV is an enveloped virus with a ss 9.6-kb RNA genome of positive-stranded polarity (195). The 5′ non-translated region of the genome contains an internal ribosome entry site (IRES) that directs translation of a single long reading frame (196–198).

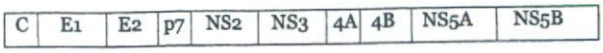

Fig. 1. Schematic representation of the HCV genome.

The HCV open reading frame (ORF) encodes a single polyprotein that is 3008–3037 amino acids in length and is post-translationally modified to produce at least 10 different proteins: core, the envelope proteins E1 and E2, p7, and the non-structural proteins NS2, NS3, NS4A, NS4B, NS5A, and NS5B (Fig. 1) (162,199). These viral proteins are not only involved in viral replication but may also affect a variety of cellular functions (162,200). Based on nt sequence comparisons, HCV genomes can be grouped into at least six genotypes, or clades, that differ from each other by 31–34%. Furthermore, several subtypes have been defined, with an nt sequence diversity of ≈20%. HCV has infected an estimated 170 million people worldwide, making it a global health problem (201). HCV is one of the main causes of liver-related morbidity and mortality; it establishes a persistent infection of the liver, leading to the development of chronic hepatitis, liver cirrhosis, and HCC (202). It is estimated that 40–60% of infected individuals progress to chronic liver disease, with many of these patients ultimately requiring liver transplantation (203). At present, HCV infections can be treated with IFN-β, either alone or in combination with ribavirin. Standard therapy has a poor response rate (204), and thus alternative therapeutic approaches for chronic HCV are needed. To overcome this situation, a number of groups have attempted to verify the usefulness of RNAi as a therapeutic tool in several model systems, as described below. The findings indicate that siRNA and shRNA against HCV interfere efficiently with HCV gene expression and replication.

McCaffrey et al. (205) investigated the effect of siRNA and plasmids expressing shRNA against HCV NS5B on the expression of an HCV NS5B fragment fused with luciferase RNA in mouse liver using hydrodynamic injection. Quantitative whole-body imaging showed that siRNA and shRNA decreased luciferase expression by 75% and 90%, respectively.

Wilson et al. (206) investigated the effect of siRNA on the expression of HCV-specific proteins and RNA synthesis in Huh cells containing an HCV subgenome replicon. siRNA against NS5b and NS3 inhibited expression of NS3 and NS5b protein and reduced HCV replicon RNA levels by >94%. These siRNAs protected native Huh7 cells from challenge with HCV replicon RNA by >95%. Treatment of the cells with the siRNAs was effective for >72 h, but the duration of RNAi treatment could be extended beyond 3 weeks through stable expression of complementary strands of siRNA under the control of two separate H1 promoters by using a vector. The vector-based siRNA protected native Huh7 cells from challenge with HCV replicon RNA by 70%.

Wilson et al. (207) wondered whether the small percentage of surviving Huh cells challenged with HCV replicon were resistant to RNAi in general or to the specific siRNA being used. After several treatments with a highly effective siRNA, growth of replicon RNAs resistant to subsequent treatment with the same siRNA was observed. Sequence analysis of the siRNA-resistant replicon showed the generation of point mutations within the siRNA target sequence. Use of a combination of two siRNAs severely limited escape mutant evolution.

Kapadia et al. (208) investigated the effect of siRNA, NS3-1948, and NS5B-6133 (named on the basis of their nt location in subgenomic replication) on ongoing HCV replication and protein expression in Huh7 cells that stably replicate HCV RNA. siRNAs decreased HCV replication ≈20-fold. The RNAi effect was effective for at least 6 days. siRNAs decreased NS3 and NS5B proteins on Day 4. The siRNAs induced several IFN-induced genes to a much lesser extent compared to IFN, suggesting that the inhibition of HCV replication was not due to dsRNA-induced activation of the IFN pathway. siRNAs did not affect the cell cycle, suggesting that inhibition of HCV replication was not due to an effect on cell-cycle progression.

Randall et al. (209) investigated the effect of siRNA against 5′ core and NS4B regions on the NS5B protein, as well as cytoplasmic replication of HCV RNA in Huh7.5 cells containing HCV-Con1 and HCV-C/LB. HCV-Con1 is a full-length genotype 1b replicon with a highly adaptive serine to isoleucine substitution at amino acid 2204 of the HCV polypeptide. This has previously been described as Con/F1-neo (S22041) (210). HCV-C/LB is a chimeric replicon in which Con1 sequences, including part of NS3, all of NS4A, -4B, and -5A, and part of NS5B, were replaced with the corresponding region from the genotype 1b LB strain. siRNA against the 5′ core region (siHCV) decreased NS5B protein to an undetectable level in HCV-Con1 and HCV-C/LB cells on Day 4. siRNA against the NS4B region also decreased the NS5B protein to an undetectable level in HCV-Con1 cells, but not in HCV-C/LB cells. siHCV decreased the HCV RNA level 80-fold at Day 4 in the HCV-Con1 cells, and this level was maintained after 4 days. siHCV decreased the number of NS5A staining cells by >99%. Randall et al. also assessed the efficacy of siHCV in clearing Huh7.5 cells of replicating full-length HCV. The measurement was based on the